



Norwegian University of
Science and Technology

Seismic data interpretation of the Snøhvit gas field

Joao Silva Leonardo
Unguana

Petroleum Geosciences

Submission date: Januar 2016

Supervisor: Egil Tjøland, IPT

Norwegian University of Science and Technology
Department of Petroleum Engineering and Applied Geophysics



NORGES TEKNISK-NATURVITENSKAPELIGE UNIVERSITET

FACULTY OF ENGINEERING SCIENCE & TECHNOLOGY

DEPARTMENT OF PETROLEUM ENGINEERING AND

APPLIED GEOPHYSICS

**MAPPING OF THE RESERVOIRS AND DETAILED MODELLING OF
HYDROCARBONS IN THE SNØHVIT FIELD**

Student Name:

João Silva Leonardo Unguana

**“All the models are wrong but some are useful. (...) Is the model illuminating and useful”?
(George Box, 1978)**

Abstract

In this work, 3D seismic and well data are used for mapping the Snøhvit reservoir and modelling the hydrocarbon column through Petrel software. The reservoir mapping procedure consisted in interpreting horizons, faults and other relevant features. This mapping and modelling process have been done after exporting and calibrating the data.

The data calibration consisted of tying seismic to well data. This had been done using check shots (well data) to produce a Time Depth Relationship (TDR) and, thereafter, mimic the seismic data at well location, i.e. produce a synthetic seismogram for the 7121_6_1, 7121_4_1 and 7121_5_1 wells all, inside the cube. The seismograms were used through a local comparison with seismic data followed by adjustment to bring coincidence in real and convolved seismic data.

Later on, the Time Depth Relationship was used to build the velocity model which have been used to convert objects (interpreted well top surfaces, fluid contacts surfaces) in forward direction, i.e. time to depth domain.

Finally, using the interpreted fluid contacts Isopachs should be produced for the three different structures. This was not done due to the time constraints.

Acknowledgements

I would like to express my gratitude to Professor Egil Tjøland, for being my supervisor when I returned to NTNU, Norway after the attempt of working from home, Mozambique.

So many institutions and people have contributed in for this result of more than two year studies; the NTNU and UEM universities, Statoil enterprises, ENH, Project Coordinator, colleagues and others.

The person who has been working hard to help on the Petrel software, Dicky Harishdayat, I would like to thank him for the time used for introducing me into the software.

Studying abroad requires huge financial investment from travelling expenses up to university fees taxes.

Therefore, I would also like to thank the Eduardo Mondlane University, Cooperation Department in especial for helping through financial support in addition to Statoil along the master degree studies.

Stay away, more than 10 000 km from home, is a challenge for one who has never been far a tenth of the distance involved.

Nothing of this would be possible if my family, in Mozambican context, had not given a spiritual stability and had not invested on me throughout the years; for them I want to dedicate this work.

Table of Content

Abstract.....	i
Acknowledgements.....	ii
Table of Content	iii
List of Figures	v
List of Table	vi
1. Introduction	1
2. Work flow of the thesis.....	2
3. Geological background of the Barents Sea Area.....	2
3.1 The Barents Sea geological setting	3
3.2 The evolution of the Western Barents Sea	4
3.3 The Hammerfest Basin and the Snøhvit field	8
3.4 The stratigraphy and deposition system in Hammerfest basin	9
3.5 The structural geology of the Hammerfest Basin	10
3.6 The reservoirs in the Snøhvit Gas Field.....	11
4. Database	13
4.1 Seismic data	15
4.2 Well data	15
5. Results.....	17
5.1 Interpreted horizons	18
5.1.1 The Top Hekkingen Surface	19
5.1.2 The Top Stø Formation.....	20
5.1.3 The Top Nordmela Formation.....	21
5.1.4 The Top Tubåen Formation.....	22
5.2 Interpreted faults.....	23
5.3 Reservoir signature	26
5.3.1 Gas-Oil and Oil-Water Contacts in the reservoir	28
5.4 Velocity Model in the reservoir interval	34
6. Discussion.....	35
7. Conclusion.....	37
8. Reference	38
Appendix	39

The composite logs	40
The composite logs in the reservoir area	44
The Synthetic Seismogram.....	48
The Fluid contacts in the interpreted structures inside the cube	53

List of Figures

Figure 1: The stages undergone on the thesis.	2
Figure 2: The location of the South western Barents Sea and the Snøhvit field in the Hammerfest. From (Mohammedyasin, 2015).....	4
Figure 3: The main geologically events and stages in the Barents Sea particularly in the Hammerfest Basins and surrounding nearest area. Adapted from (Faleide et al., 1984).....	6
Figure 4: The different evolution events of the Hammerfest Basin and the nearest structural elements. From (Faleide et al., 1984).....	7
Figure 5: The location of the discovery well in the semihorst, Snøhvit gas field. The horizons are laterally interrupted due to the normal faults in the area. Adapted from (Linjordet and Olsen, 1992)...	9
Figure 6: Sketch of the section trough Finnmark Platform, Hammerfest Basin and Loppa High. From (Mohammadasy, 2015)	11
Figure 7: The wells location the in the Snøhvit Field. The seismic lines (not shown here) have a South - North (cross lines) and East –west (In lines) orientation.....	13
Figure 8: The well sections windows showing the result of the convolution model using 7120/6-1 well data.....	14
Figure 9: The composite logs for the 2720/6_1 well. Some well Formations top are displayed.....	16
Figure 10: The gas Chimney effect on the in-line 2255 and in the Seeding 3D Auto-tracking interpreted Hekkingen Surface.....	18
Figure 11: The Top Hekkingen Surface; a Seeding 3D auto tracking and b the corresponding smoothed surface.	20
Figure 12: The Top Stø Surface; a Seeding 3D Auto-tracking and b the corresponding smoothed surface.....	21
Figure 13: The Top Nordmela Surface; a Seeding 3D auto tracking and b the corresponding smoothed surface.....	22
Figure 14: The Top Nordmela Surface; a Seeding 3D auto-tracking and b the corresponding smoothed surface.....	23
Figure 15: The normal principal faults, assigned indices A and antithetic faults assigned indices B and the <i>Gas Chimney</i> area in red inside the cube.	25
Figure 16: The reservoir signature in the Snøhvit Field for well 7120_4_1. In the second track the deep blue, light and black colours represent respectively deep, medium shallow resistivity.	27
Figure 17: The four interpreted horizons in the Snøhvit field. All have been interpreted as a peak except the Tubåen Formation.....	36

Figure A 1: The 7120_5_1 wells composite log in the Snøhvit field. The logs initiate at the 260 meters depth.....	40
Figure A 2: The 71720_6_1 wells composite log in the Snøhvit area. The logs initiate at about 325 meters depth.	41
Figure A 3: The 7121_4_1 wells composite log in the Snøhvit area. The logs initiate at about 349 meters depth.	42
Figure A 4: The 7121_5_1 wells composite log in the Snøhvit area. The logs initiate at about 285 meters depth.	43
Figure A 5: The composite log in the reservoir interval for the well 7120_5_1.....	44
Figure A 6: The composite log in the reservoir interval for the well 7120_6_1.....	45
Figure A 7: The composite log in the reservoir interval for the well 7121_4_1.....	46
Figure A 8: The composite log in the reservoir interval for the well 7121_5_1.....	47
Figure A 9 : The well section window showing synthetic seismogram generated from 7120_5_1 well data and the wavelet obtained from statistical method, the convolution model.	49
Figure A 10 : Well section window showing synthetic seismogram generated from 7120_6_1 well data and the wavelet obtained from statistical method, the convolution model.	50
Figure A 11: Well section window showing synthetic seismogram generated from 7121_4_1 well data and the wavelet obtained from statistical method, convolution model.....	51
Figure A 12: The well section window showing synthetic seismogram generated from 7121_5_1 well data and the wavelet obtained from statistical method. The red asterisk in the correlation track shows the quality of the correlation within each trace.	52

List of Table

Table 1: The summary of some Snøhvit parameters.....	12
Table 2: The fluid contacts for both well and seismic data.....	28

1. Introduction

Since the Barents Sea seismic data were made available, it has been extensively used for diverse studies purposes.

For instance, (Ronnevik et al., 1982) used seismic data and wells to recognise different sequence in the Barents Sea, (Faleide et al., 1984) integrated reflection and refraction seismic data with gravity and magnetic to study the evolution of the Western Barents Sea during the post Caledonians times, (Ritzmann and Faleide, 2007) integrated the three types of reflectivity on the Barents Sea`s seismic data below the sedimentary rock with gravity and magnetic anomalies to describe and relates the corresponding geology units and (Mohammedyasin, 2015) used 3D seismic data to analyse the history of the fault growth and hydrocarbon leakage in the Snøhvit Field, Hammerfest Basin. Through these and other studies some conclusions listed below have been made;

The established Middle Jurassic play type is relevant for the Hammerfest basin, western flank of the Loppa Ridge and Bjørnøy Basin. (Ronnevik et al., 1982)

Geologically the Barents Sea comprises a large epicontinental sea bounded by young passive continental margin in the north and west. It`s divided into three regional geological provinces: (1) an east–west trending basinal province between 74°N and the coast Norway; (2) an elevated platform area to the north towards Svalbard; and (3) the western continental margin (Faleide et al., 1984) see figure 2.

The distribution of the oil and gas in the basin is strictly related to the burial history which involves uplift, erosion, and renewable burial in the Tertiary. (Linjordet and Olsen, 1992)

The Southwest Barents Sea geometry was inherited to the rifting history. (Ritzmann and Faleide, 2007)

Six major deep seated faults extending from the Upper Carboniferous to Eocene rocks are linked with hydrocarbon migration in the Snøhvit Field, Hammerfest Basin. (Mohammedyasin, 2015)

In this work, high quality 3D seismic and well data integrated with other relevant information are used to map Snøhvit reservoirs and, further, to evaluate the corresponding quantity of hydrocarbon through Petrel software.

2. Work flow of the thesis

There are several stages undergone throughout the work for better data judgements. Here only the main stages, which include: a. Integration of the data through Petrel@2015; b. Sonic calibration and synthetic seismogram generation, c. Mapping of the fault and horizons, d. Modelling and interpretation of gas/oil leg are described. All the stages were performed through the Petrel software.

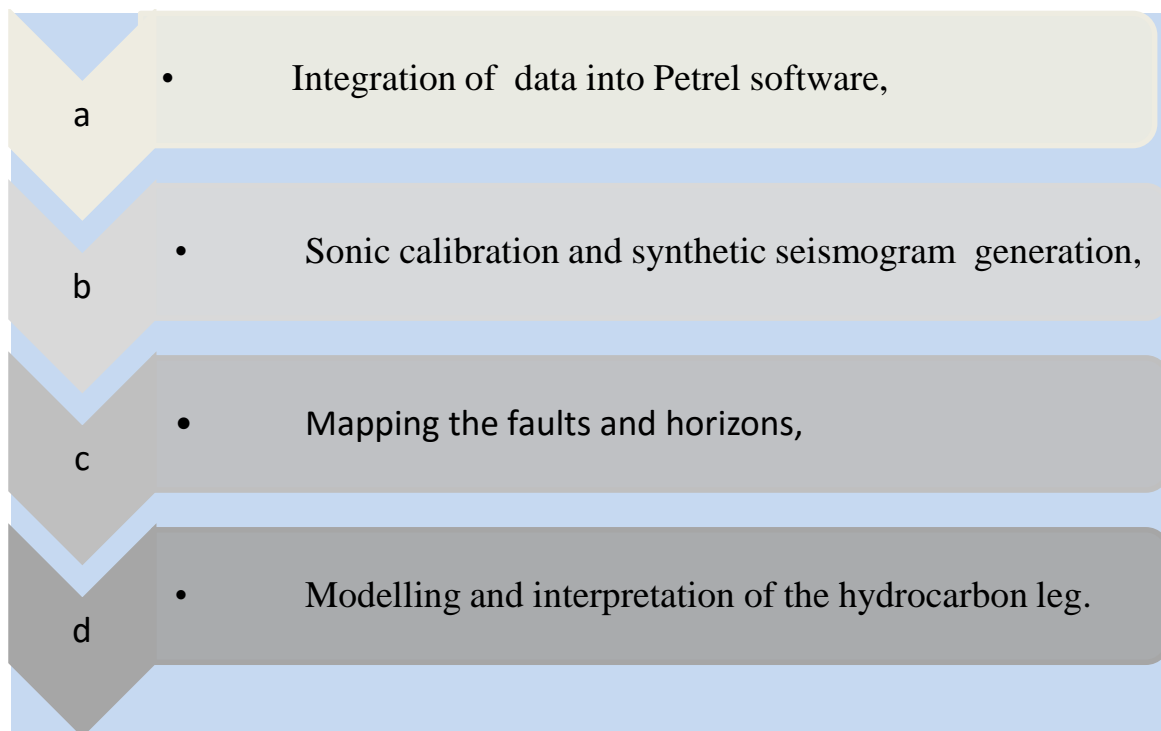


Figure 1: The main stages undergone on the thesis.

3. Geological background of the Barents Sea Area

This part of the thesis contains summarised information from the literatures listed in the references. This information is organized in relevant items; The Barents Sea geological settings, The evolution of Western Barents Sea, The Hammerfest basin and the Snøhvit field, The stratigraphy and deposition system in the Hammerfest basin, The structural geology of the Hammerfest basin and the reservoir in the Snøhvit Gas Field as an insight into the study area.

3.1 The Barents Sea geological setting

The Barents Sea has an intracratonic setting and had been affected by several phases of tectonism since the Caledonian Orogenic movements which terminated in early Devonian times, see figure 3. (Gabrielsen et al., 1990)

The crystalline basement of the Western Barents Sea is interpreted to consist of Caledonian igneous and metamorphic rocks with an Archean – Proterozoic protolith, although young volcanic are also present. (Ritzmann and Faleide, 2007)

There is carbonate and evaporites deposition in local basin belonging to Upper Carboniferous to Lower Permian.(Larsen, 2005)

According to (Clark et al., 2014) the existing carbonate rocks may be found in Bjarmaland, Tempel Fjorden and Nygrunnen group belonging to Late Carboniferous to Lower Permian, Upper Permian and Late Cretaceous respectively. The continental sand is embedded into Carboniferous and Triassic to Mid Jurassic continental shale mainly belonging to Billefjorden, Sassendelen and Kapp Toscana groups.

Structurally the Barents Sea continental shelf is dominated by ENE-WSW to NE-SW and NNE-SSE trends with a local influence of WNW-ESE striking elements. In the southern part, a zone dominated by ENE-WSW trends defined by major fault complex bordering Hammerfest and Nordkapp Basins, see figure 2 and figure 6. This trend is subparallel to another major zone to the north defined by Velesmøy High and fault complexes separating Loppa High from Bjørnørnia Basin. N-S trends prevail to the west and northwest (the Tromsø basin, Knølegga Fault and Hornsund fault Complex). (Gabrielsen et al., 1990)

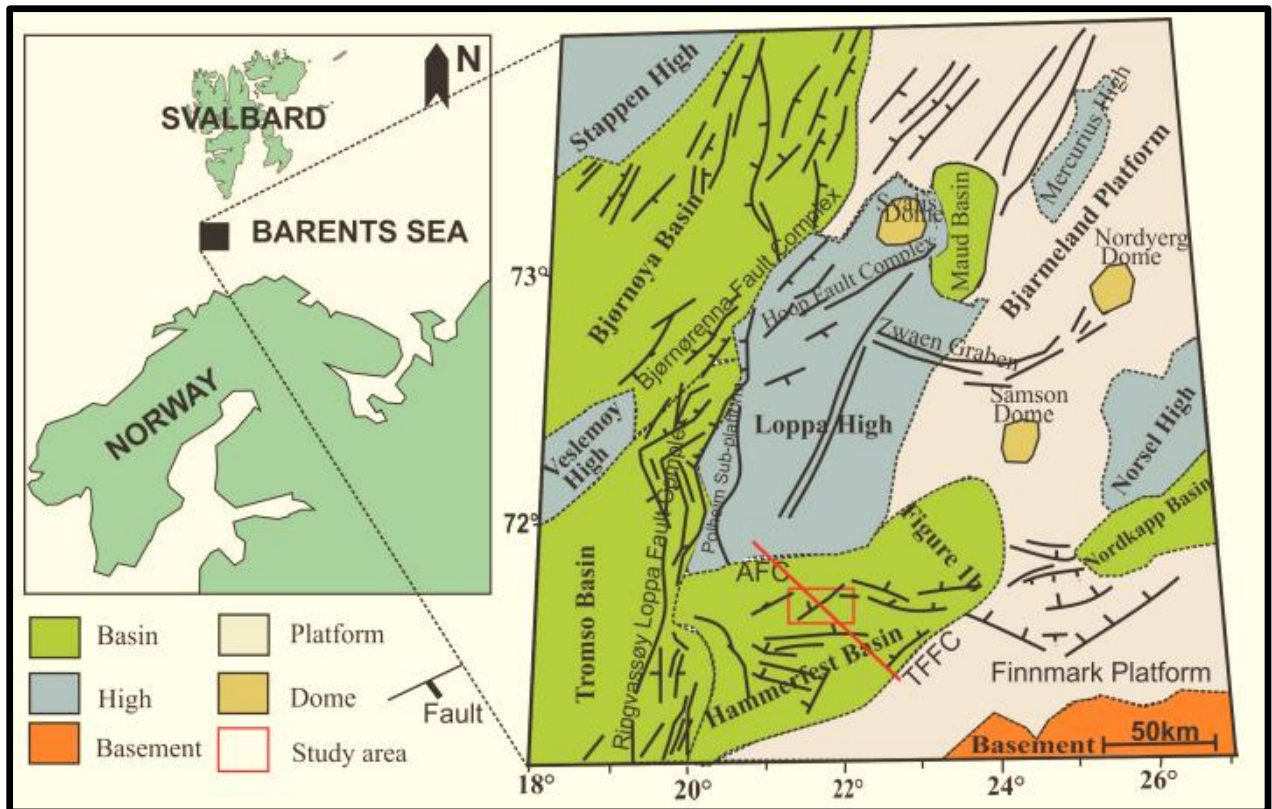


Figure 2: The location of the South western Barents Sea and the Snøhvit field in the Hammerfest. From (Mohammedyasir, 2015)

3.2 The evolution of the Western Barents Sea

The past stages, illustrated in the figure 3, at the Barents Sea encompasses: the Caledonian (A) which span from L. Silurian to Early Devonian; the Svarbadian – Ellesmerian (B) in the Late Devonian; the Hecianian-Variscan (C) in the Permo – Carboniferous, the Kimmerian (D) in Late Jurassic to Cretaceous and the Laramide (E) in Paleocene. (Faleide et al., 1984). In this figure the arrows indicate uplift and subsidence when pointing upward and downward respectively. Opposed arrows indicate a fault.

The important events which have influenced Hammerfest basins and near surrounding area's deposition system and structural geology are described;

The Caledonides were consolidated during the Late Silurian to Early Devonian Caledonian Orogeny, resulting in the suturing of the North America – Greenland and Fennoscadian – Russian Plates. (Faleide et al., 1984)

During the Late Palaeozoic most of the Barents Sea was affected by crustal extension, resulting in a fan shaped array of fault block basins separated by highs. (Faleide et al., 1984)

In the Late Devonian Caledonian compressional regime changed to a left lateral shear regime with large – scale strike-slip movements. (Ziegler, 1978)

The rift basins may have been formed along an axis from the Tromsø to the Nordkapp basins. (Faleide et al., 1984)

The Hercynian tectonic events seems to not have influenced the Western Barents Sea, whereas in the eastern part (Novaya Zemlya) in Late Permian – Early Triassic it has culminated with Formation of a mountain range.

At the end of Early Carboniferous the Barents Sea level decreased. Through Middle Carboniferous – Lower Permian, in most Barents Sea area there was little or no tectonic activity (Faleide et al., 1984) and as a result, the deposition of the Carboniferous sediment was made in a quite environment.

The Kimmerian phase includes the disintegration of the Pangea mega - continent. The Kimmerian tectonics represents rifting in discrete pulses, spanning the Rhaetian – Valanginian time interval, along the entire Arctic – North Atlantic rift system that gradually opened during the Mesozoic leading to crustal separation between the North American – Greenland and the European plates in the Early Tertiary. (Talwani and Eldholm, 1977)

However, on the Barents Sea only the Late Kimmerian tectonic regime during the transition of Jurassic - Cretaceous created series of large deep-seated normal faults along the zones of weakness in the Caledonian basement. The Ringvassøy - Loppa Fault complex in the hinge zone in South-Western Barents Sea is an example of the normal faults created. (Talwani and Eldholm, 1977)

Rifting subsidence started to increase progressively in the Barents Sea and between Norway and Greenland a period following the Late Kimmerian. (Faleide et al., 1984)

In the west, strong differential subsidence led to the Formation of the main structural elements from Stappen High to the Tromsø - Finnmark Fault Complex. The Loppa High was inverted between the subsiding Bjørnøya and Hammerfest basin. The rate of subsidence at this stage was much faster to the west of Ringvassøy – Loppa Fault Complex than on the east side. (Faleide et al., 1984)

During the Tertiary major part of the Barents Sea was uplifted and acted as a source area for clastic wedge along the western margin.

The Hammerfest and Nordkapp Basins were uplifted and the Upper Cretaceous was eroded during Laramide phase near base of Tertiary. (Ronnevik et al., 1982)

These events have transformed gradually the subsurface area to the today basin and platforms as it's illustrated in a NW to SE and N NE to SSE in the figure 4.

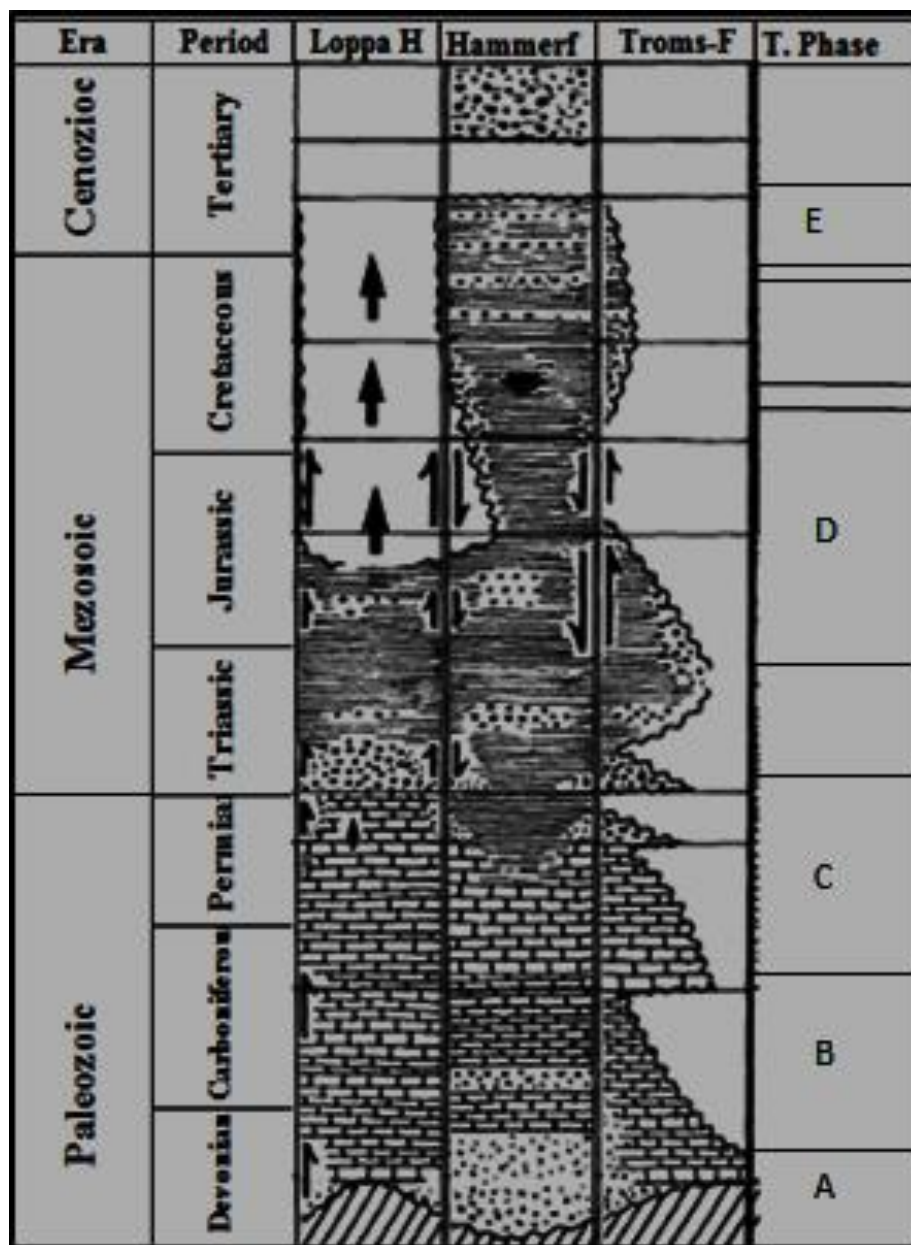


Figure 3: The main geologically events and stages in the Barents Sea particularly in the Hammerfest Basin and surrounding nearest area. Adapted from (Faleide et al., 1984)

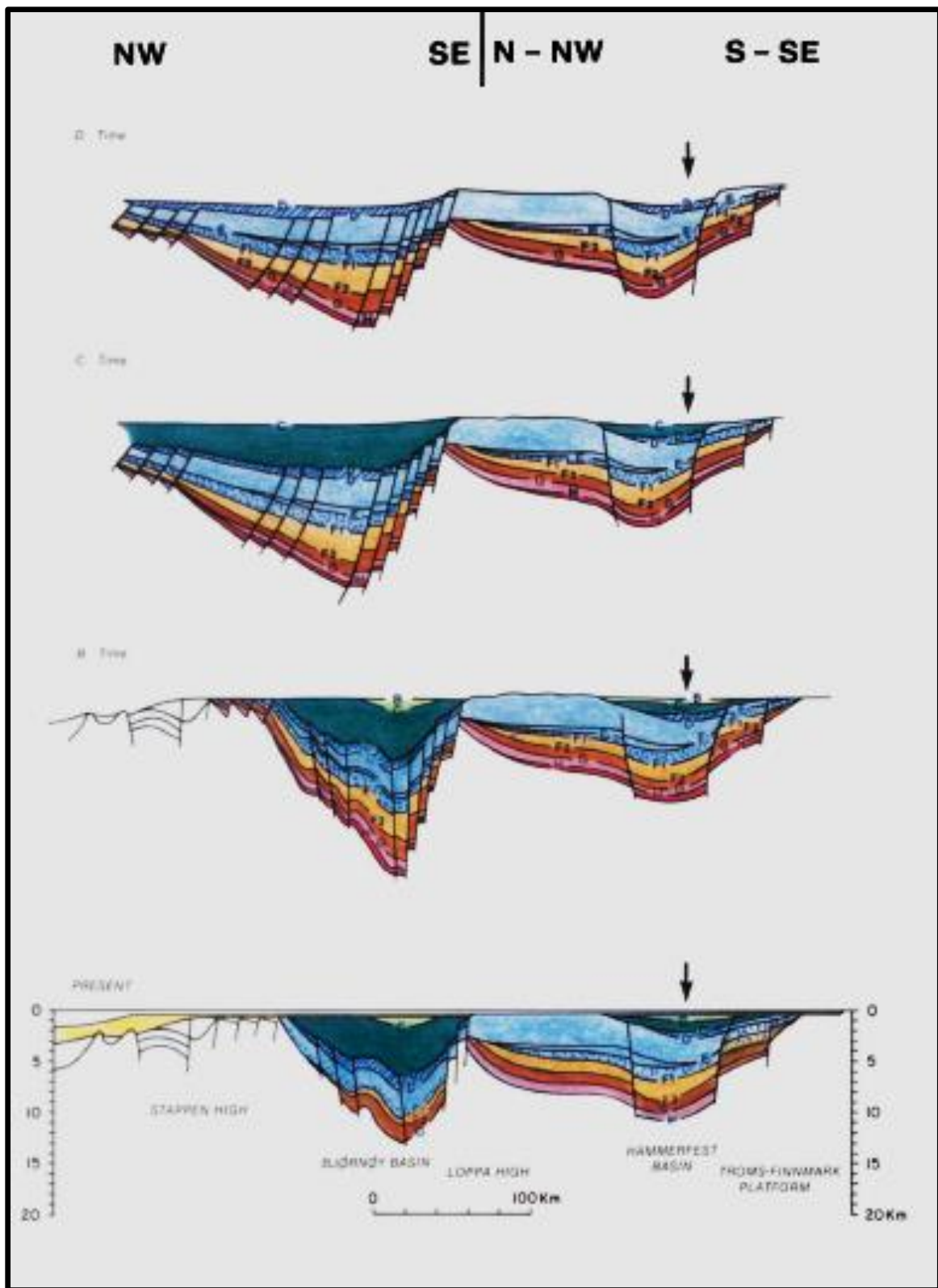


Figure 4: The different evolution events of the Hammerfest Basin and the nearest structural elements. From (Faleide et al., 1984)

3.3 The Hammerfest Basin and the Snøhvit field

The Hammerfest basin has been interpreted as a failed rift in triple junction. (Talleraas, 1979 in (Gabrielsen et al., 1990))

It is situated between Loppa High and Finnmark Platform in the NW - SE orientation (see figure 2 and figure 5) and, it is separated from the Finnmark Platform to the south by Tromsø – Finnmark Fault Complex and from Loppa High to the North by Asterias Fault Complex.

Its western limitation toward Tromsø Basin is defined by the southern segment of the Ringvassøy – Loppa Complex, while the eastern border has the nature of a flexure against the Bjarmaland Platform, figure 2.

The basin may be divided into two parts; western and eastern sub basin separated by extensional by Trollfjord-Komagelev fault trend. The western part dips westward toward Troms. (Gabrielsen et al., 1990)

This basin, according to Berglund et al. 1986 in (Gabrielsen et al., 1990), it may have been initiated by extensional tectonics in the Carboniferous.

The Snøhvit gas field is situated almost in the centre Hammerfest basin with the reservoirs situating in two smaller “semihorst”, in the east and northwest, see figure 4.

It covers 90 km² and has a 124 m gas column overlying a thick 14 m oil leg. See table 1 for the Oil- Water Contact (OWC) and Gas-oil contact (GOC) depth suggested by literatures.

The major portion of hydrocarbon in it is encountered in the Stø Formation and about a tenth in Nordmela Formation. (Linjordet and Olsen, 1992)

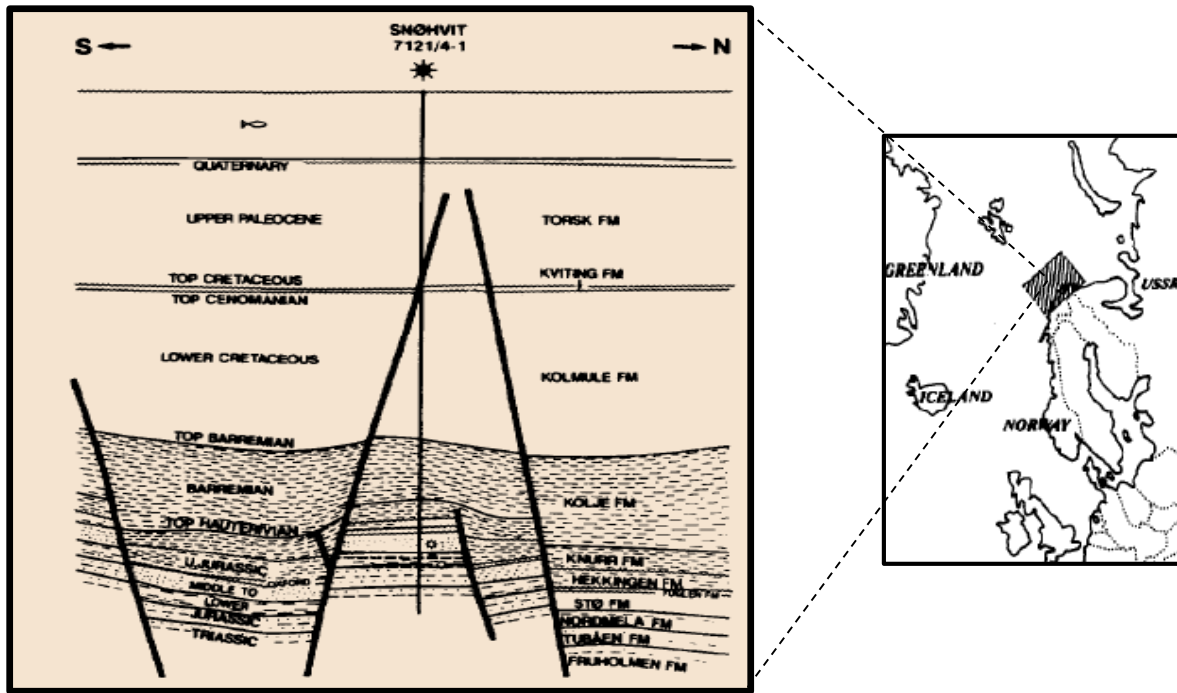


Figure 5: The location of the discovery well in the semihorst, Snøhvit gas field. The horizons are laterally interrupted due to the normal faults in the area. Adapted from (Linjordet and Olsen, 1992)

3.4 The stratigraphy and deposition system in Hammerfest basin

The Hammerfest basin contains 5000 m of strata above the basement in the Snøhvit Field;

The Middle to Upper Triassic strata are characterized by a lower sequence of interbedded shales that are occasionally carbonaceous and contain coal fragments overlain by shale and silty unit that has increasingly more interbedded sandstone upward, these sediments have been interpreted as been deposited in a deltaic environment. (Linjordet and Olsen, 1992)

The Lower to Middle Jurassic strata consist mainly of sandstone interbedded with thin shale layers deposited in a shallow marine coastal plain environment with fluctuation coastlines. Tubåen Formation has thick sandstone with shale beds which are in parts carbonaceous these sediments are interpreted as representing an estuary environment. (Linjordet and Olsen, 1992)

The 1200 m Cretaceous sediments were deposited in a marine – shelf environment. The strata consist mainly of claystone with thin sandstone and siltstone stringers. In parts of the same area limestone and dolomite occur and occasionally the limestone is interbedded with claystone. (Linjordet and Olsen, 1992)

In the marine shelf with restricted bottom water conditions environment, about 600 m of Palaeocene to Eocene claystone containing Stringers of sand, siltstone, limestone and dolomite and traces of tuff exist at a base of Tertiary sequence.

There are hiatus from Upper Jurassic to Lower Cretaceous, from lower to Upper Cretaceous and upper tertiary sequence. In the tertiary, Pliocene to Pleistocene sequence is only represented by only 100 m. (Linjordet and Olsen, 1992)

3.5 The structural geology of the Hammerfest Basin

The Hammerfest Basin is a Late Kimmerian trough trending east - northeast and lying among the Loppa High to the north, the Tromsø basin to the west and Tromsø Finnmark platform to the south. The basin is symmetrical, but widens deep westward and it is surrounded by Tromsø - Finnmark Fault Complex and Asterias Fault Complex as is shown on the figure 2 and figure 6.

The dominant east – west trending fault system in the central part of the basin was formed by flexural extension related to the doming.

According to (Mohammedyasin, 2015) in the Snøhvit there are six major faults which are characterized by complex lateral and vertical segmentation. These faults are affected by three main episodes of fault reactivation in Late Jurassic, Early Cretaceous and Palaeocene times. He also argues that there is interaction between the faults within sedimentation through their growth history.

Today geological section crossing the Hammerfest Basin in NW-SE direction is shown in the Figure 6.

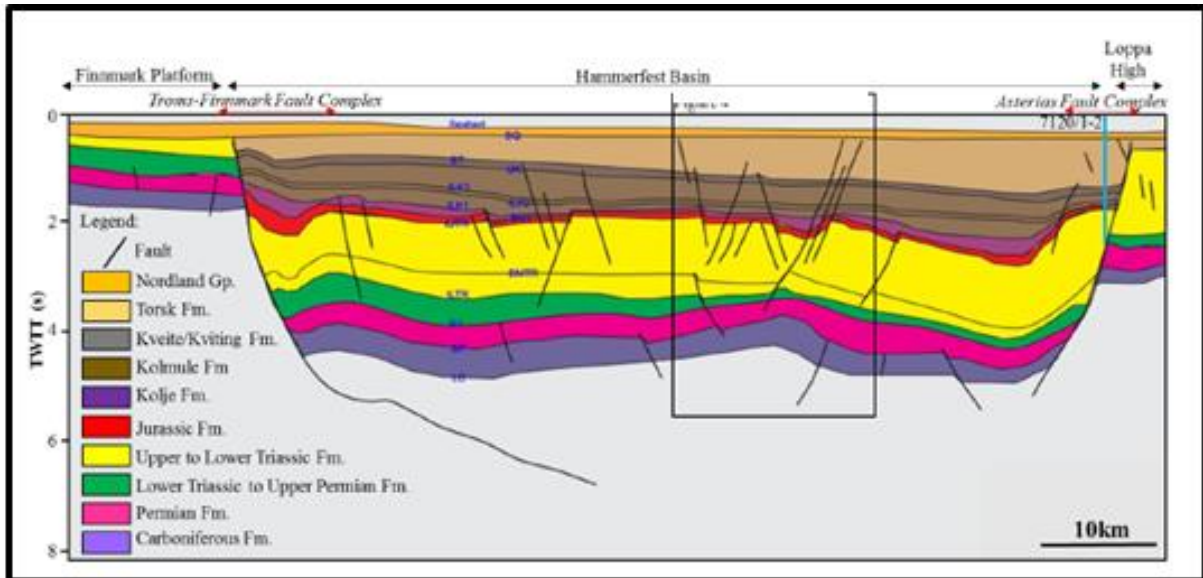


Figure 6: The sketch of the section trough Finnmark Platform, Hammerfest Basin and Loppa High. From (Mohammedyasin, 2015)

3.6 The reservoirs in the Snøhvit Gas Field

In the Snøhvit gas field the reservoir are the Jurassic Stø and Nordmela formations. The sandstone of the Lower to Middle Jurassic Stø and Nordmela formations are generally well sorted and medium to fine – grained, and exhibit various degrees of rounding. (Linjordet and Olsen, 1992).

According to (Linjordet and Olsen, 1992) the Nordmela Formation was deposited in a coastal or delta plain environment with active distributary feeder channels and possible tidal channel, while the Stø sandstone Formation were deposited in an overall shallow marine settings. The alternating shales in the Stø Formation mark transgressive events in an offshore environment.

The Snøhvit which covers 90 km² contains both oil and gas; the gas column is about nine times the oil column. Below, in the Table 1, there is a summary of the Snøhvit field formations made through the literatures.

Table 1: The summary of some of the Snøhvit parameters. Adapted from (Linjordet and Olsen, 1992)

Local	Parameter	Description
Stø Formation	Lithology	Sandstone, shale
Nordmela Formation		Silty shale and sandstone
Stø Formation	Depositional environment	Shallow marine and (or) offshore environment
Nordmela Formation		Coastal or delta plain
Stø and Nordmela Formations	Gross thickness	(130 - 200) m
	Age	Early/Middle Jurassic
Snøhvit field	GOC	2404 m MSL
	OWC	2418 m MSL
	Oil column	14 m
	Gas column	124 m
	Source rock	Late Jurassic shales (Hekkingen Formation)
		Early Jurassic Nordmela Formation
		Triassic shales
	Trap	Tilted fault blocks
Seal	Fuglen and Hekkingen Formations	
GIIP	5.6 Tcf	

4. Database

The used data consist of 3D Post-Stack Time Migration (PSTM) seismic data and 7120_5_1; 7120_6_1; 7121_4_1; and 7121_5_1; well data, see figure below, integrated into Petrel® 2015.

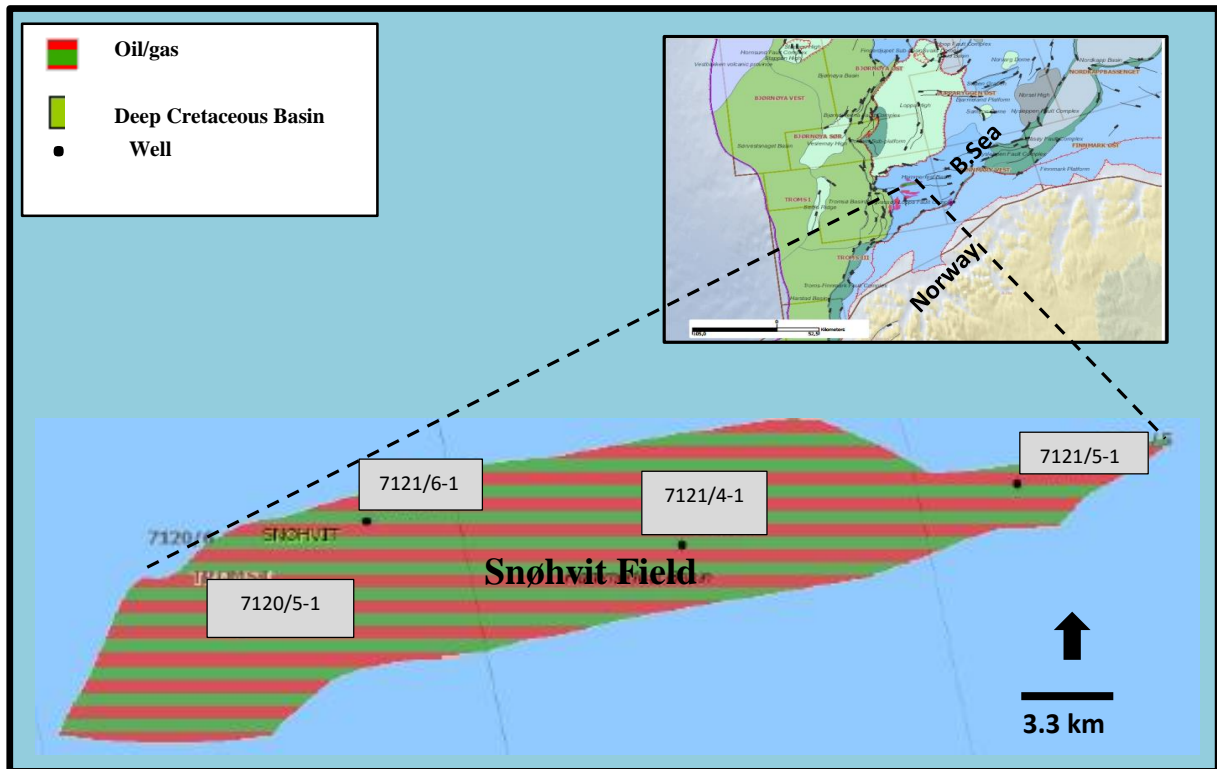


Figure 7: The wells location in the Snøhvit Field. The seismic lines (not shown here) have a South - North (cross lines) and East –west (In lines) orientation.

The wells data consist mainly of check shot data, composite log, well Top Formations and well path.

Part of the wells data have been acquired through Norge National Petroleum Directorate (NPD).

Apart from the data, there are several stages undergone for better data judgements which are listed on the work in the thesis.

Integrating data into petrel required its pre-organization in other program, mainly excel, followed by conversion into appropriate Petrel® 2015 format, so that it could be imported and visualized.

Calibrating the sonic and synthetic seismogram generation is an important stage of the well tie. Sonic log were calibrated with check shots and later on the time depth relation used for building the velocity model.

For the synthetic generation, some steps have been followed and the main steps are shown in one well, although the steps have been made for all wells.

The figure 8, below shows the synthetic seismogram generation (track 5) in the reservoir area from the well 7120_6_1 resulted from reflectivity series and the wavelet (track 3), the so called convolution model. See that in the track 1 is shown density and velocity logs used as input to obtain the reflectivity series (track 2). The correlation, in track 6, is used to show similarity between seismic data (track 4) and the seismogram. The track 7 shows the interval velocity and track 8 shows the time applied in the synthetic to best match to seismic, known as drift. The red line represents a well trajectory.

Moving the synthetic seismogram vertically best correlation had been achieved in the well 7121_4_1.

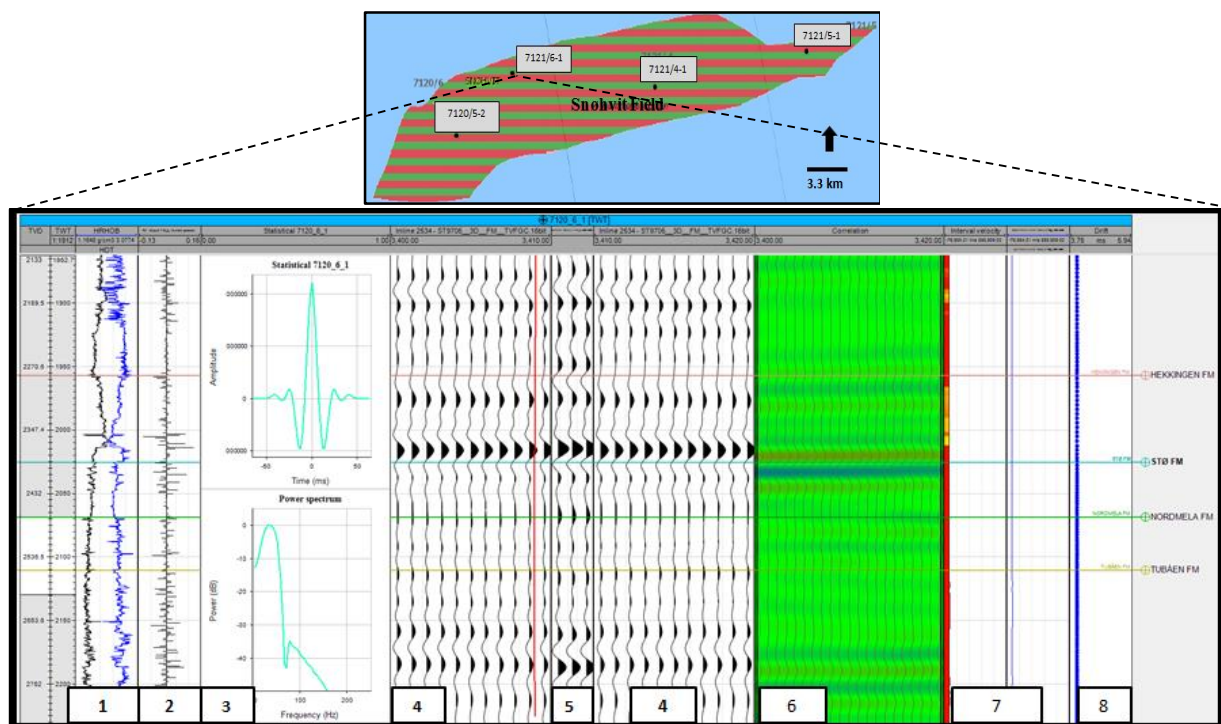


Figure 8: The well sections windows showing the result of the convolution model using 7120/6-1 well data. The tracks have been assigned ordinary number which are explained through the test.

The horizons were mapped using *Seeded 3D Auto - Tracking Seismic* horizon interpretation tool across individual seismic profiles, while the faults were interpreted manually across

seismic profiles. Manual faults interpretation are most reliable than auto tracking whereas, for horizon interpretation, the *Auto Tracking* reveals to be better.

The horizon and faulting mapping performed was not sufficient to visualise and extract attributes related to oil column. This is justified by the fact that seismic resolution is beyond the oil column in the reservoir which is less than 15 metres.

Therefore, there has been used the logs to evaluate and seismic to evaluate the oil quantity. This oil column determination is based on the fact that within a thickness (beyond seismic resolution) there are some well logs parameters that were used to study the local oil column characteristics.

4.1 Seismic data

The 3D seismic data in the study area consisting of Post - Stack Time – Migrated data cover an approximated $4.8 \cdot 10^8 \text{ m}^2$. It contains In-lines, in the north-south direction and Cross Lines in the east–west direction. The lines lengths are respectively 1.25 km and 47.100 m approximately.

The notable reflectors in the seismic sections tend to be horizontal and continuous excluding the reflectors in the reservoirs and nearest areas which are severe discrete interrupted. Some of these reflectors correspond to the Hekkingen, Stø, Nordmela, and Tubåen tops Formation.

4.2 Well data

The Snøhvit wells data shown on the figure 7 consist of the following composite log; Gamma Ray (HGR), Resistivity (HRD, HRM and HRS), Density (RHOB), Neutron Porosity (HNPHI) and Slowness (DT) logs, Calliper (HCALI) and the calculated Acoustic impedance logs. The wells are separated from each other at a distance bigger than 8 km: well 7120_ 6_1 from 7121_4_1, 8155 m; 7121_4_1 from 7121_5_1, 8745 m; and 7121_5_1 from 7120_5_1, 34150 m apart from each other.

The logs were initialised close to a top of Nordland Group reflector; in most wells between 300 m and 340 m excluding the 7120_ 5_1 which begins at about 285m True Vertical Depth (TVD), see the figure 9 and in the appendix figure A1, figure A2, figure A3, and figure A4.

They have been organised in such way to easy their interpretation and the reservoir location; the Gamma Ray log in track one, the Resistivity logs (Deep, Medium and Shallow resistivity) on track two, the Density and Neutron log on the track three and the slowness in track four. The scales have been set taking into account the common log fluctuation in the reservoirs area. There are in general similarities within the corresponding logs in different wells.

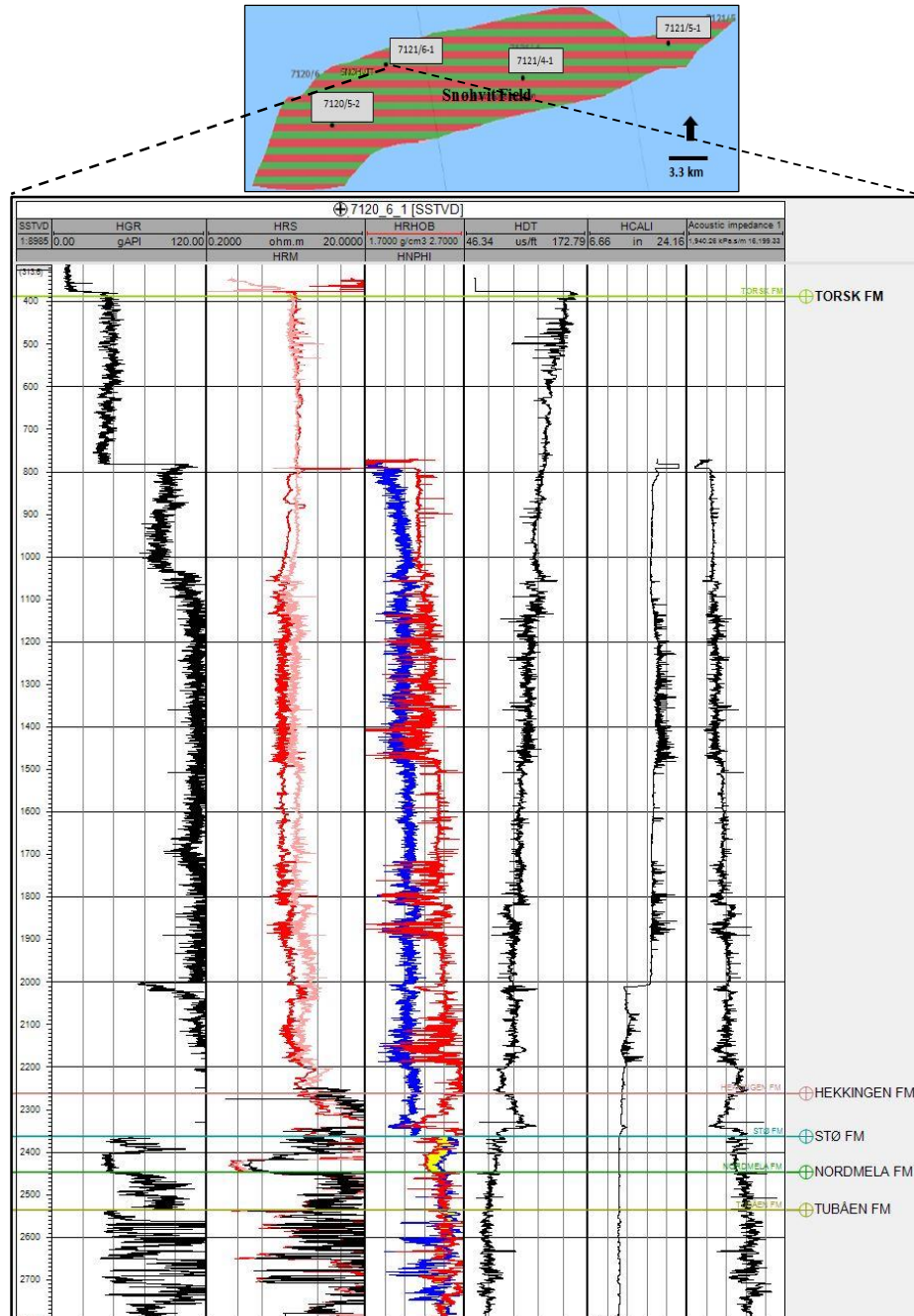


Figure 9: The composite logs for the 2720/6_1 well. Some well Formations top are displayed.

5. Results

After data calibration steps, horizons and faults have been mapped. There were seen interesting anomalies from high amplitude to dimming reflectors and inclined reflectors.

Rotation of the blocks, especially the smaller blocks, indicated by inclined reflectors in relation the surrounding make it difficult to map locally the horizons.

High amplitudes anomalies with opposite or reversed polarity to the seabed reflector are characterized as “soft reflections” i.e., fluid leakages or accumulation in the subsurface. (Alves et al., 2015)

From the Cross Line 3751 up to 4271 there is a bad data quality related to *Gas Chimney*. The *Gas Chimney* effect, additionally deteriorates the seismic data in the seismic In-lines dimming it, although it improves northward. The figure 10 shows the *Gas Chimney* (in red) on the western part of the seismic data and, in addition, the wells with a separation space of more than 8km in the cube. On the upper left side, there is a part of the un-interpreted seismic 2255 In-line showing reflectors dimming and its interruption due to the *Gas Chimney* effect. In b, on the opposite side, some of the interrupted reflectors, in the same line have been mapped and shown; the Hekkingen, Stø and Nordmela Top Formations. The bottom part of the figure, c shows the seismic cube with the *Seeding 3D Auto-Tracking* interpreted Hekkingen horizon.

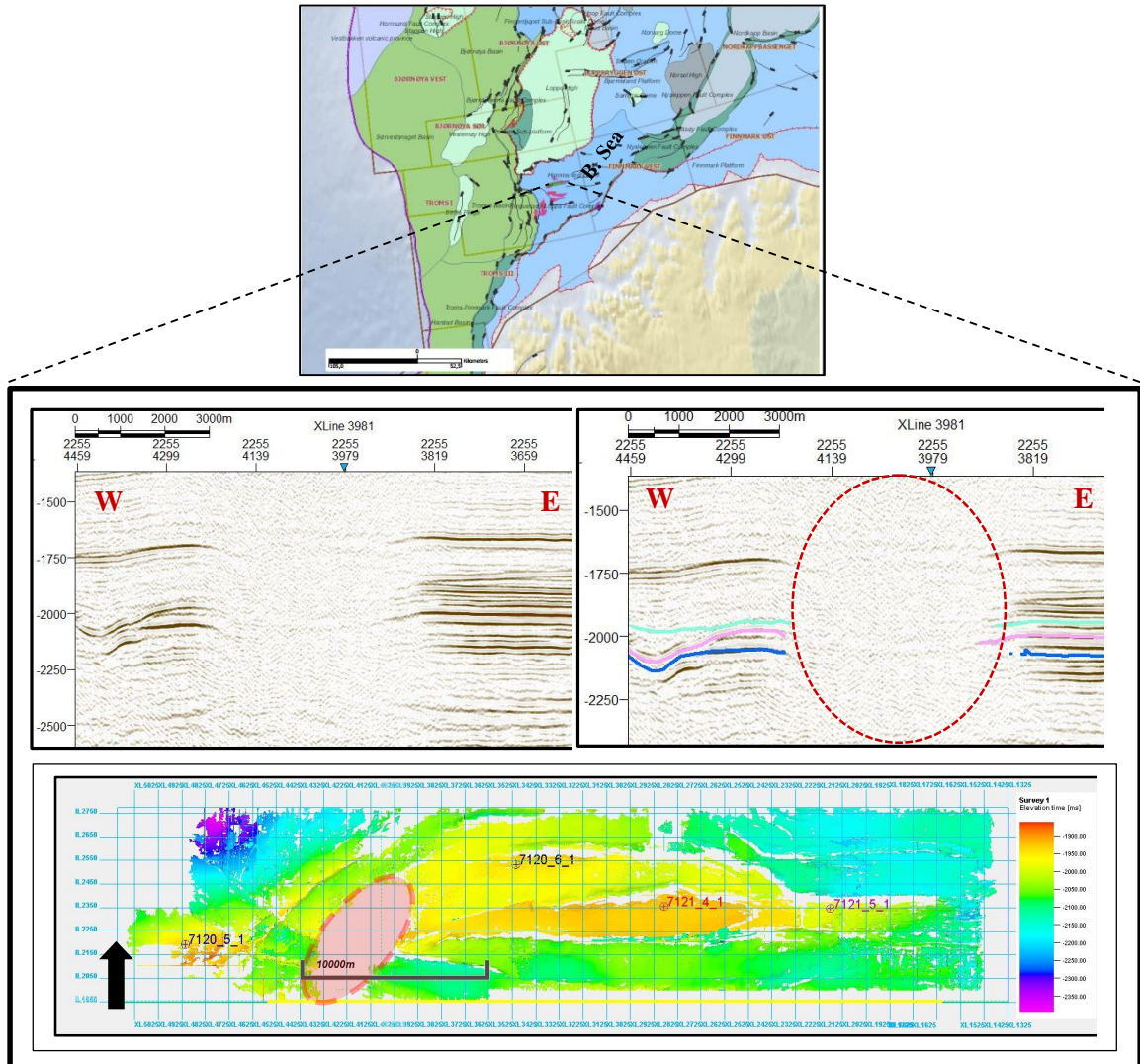


Figure 10: The Gas Chimney effect on the in-line 2255 and in the Seeding 3D Auto-tracking interpreted Hekkingen Surface.

5.1 Interpreted horizons

Four (4) horizons in the reservoir area have been mapped and, as a result the following *Seeding 3D interpreted surfaces* were obtained; the Top Hekkingen Formation Surface, the Top Stø Formation Surface, The Top Nordmela Formation Surface and the Top Tubåen Surface. These surfaces served as input to obtain the complete surfaces which, further, were smoothed to obtain clearer surface image (without spikes).

On the left part of each surface is displayed the elevation time and corresponding colour interval. The violet represents maximum wave-traveltime and therefore maximum depth whereas red represents minimum both wave-traveltime and depth.

The sharply colours change here will mean faulted surface by huge faults or sharp synclines shape while smooth colours change will mean smooth dipping and/or presence of minor faults.

Basically the surfaces are made up by 4 areas; the most elevated area in the centre, an area surrounding the centre with relatively less elevated area, north-eastern and north-western lower area and the lowest area in further north east area.

5.1.1 The Top Hekkingen Surface

The top Hekkingen Formation has larger acoustic impedance contrast in some area and, as a result, higher reflectivity. This horizon property easier it's mapping process through *Seeding 3D Auto-Tracking* and the result is shown in the figure 11,

Both *Seeding 3D Auto - tracking surface* (figure 11 **a**) and the corresponding smoothed surface (figure 11 **b**) show mainly the same characteristic except the gap resulted from the gas leakage effect which was filled by an interpolation method.

On the centre and the south-western surface part, there are the most elevated areas, whilst the south-eastern and the north-eastern part the deepest area is notable. The colours change sharply northward meaning existence of faults in opposite direction and separating the areas. Indeed, the yellow-reddish centre elevated area is surrounded by yellow and green colours.

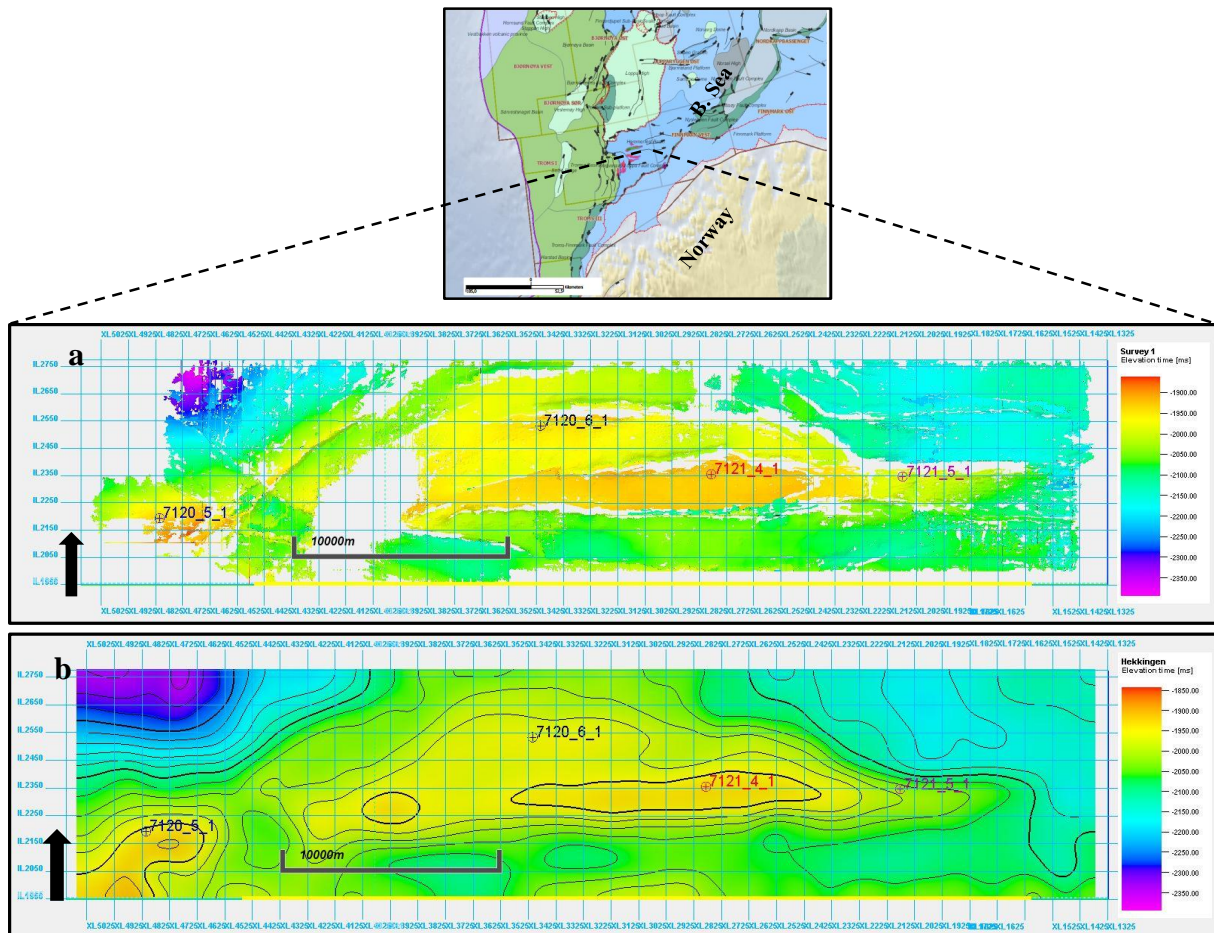


Figure 11: The Top Hekkingen Surface; **a** Seeding 3D auto tracking and **b** the corresponding smoothed surface.

5.1.2 The Top Stø Formation

The Top Stø Formation has huge acoustic impedance contrast almost in the entire cube and, as a result, huge reflectivity. Indeed, the confidence on mapping this horizon through *Seeding 3D Auto-Tracking* was higher see figure 12.

Both *Seeding 3D Auto-tracking surface* (figure 12 **a**) and the corresponding *smoothed surface* (Figure 12 **b**) show almost the same characteristic.

On the surface centre there is the most elevated area, whilst on north-eastern exist two separated synclinal shape, and on the north-western one sharp synclinal shape exist. The colours change sharply northward meaning existence of faults in opposite direction and separating the areas.

However, on the North-eastern area the gradual blue colours change is related to the smooth synclinal and the change from light blue to violet is relate to sharp synclinal shape.

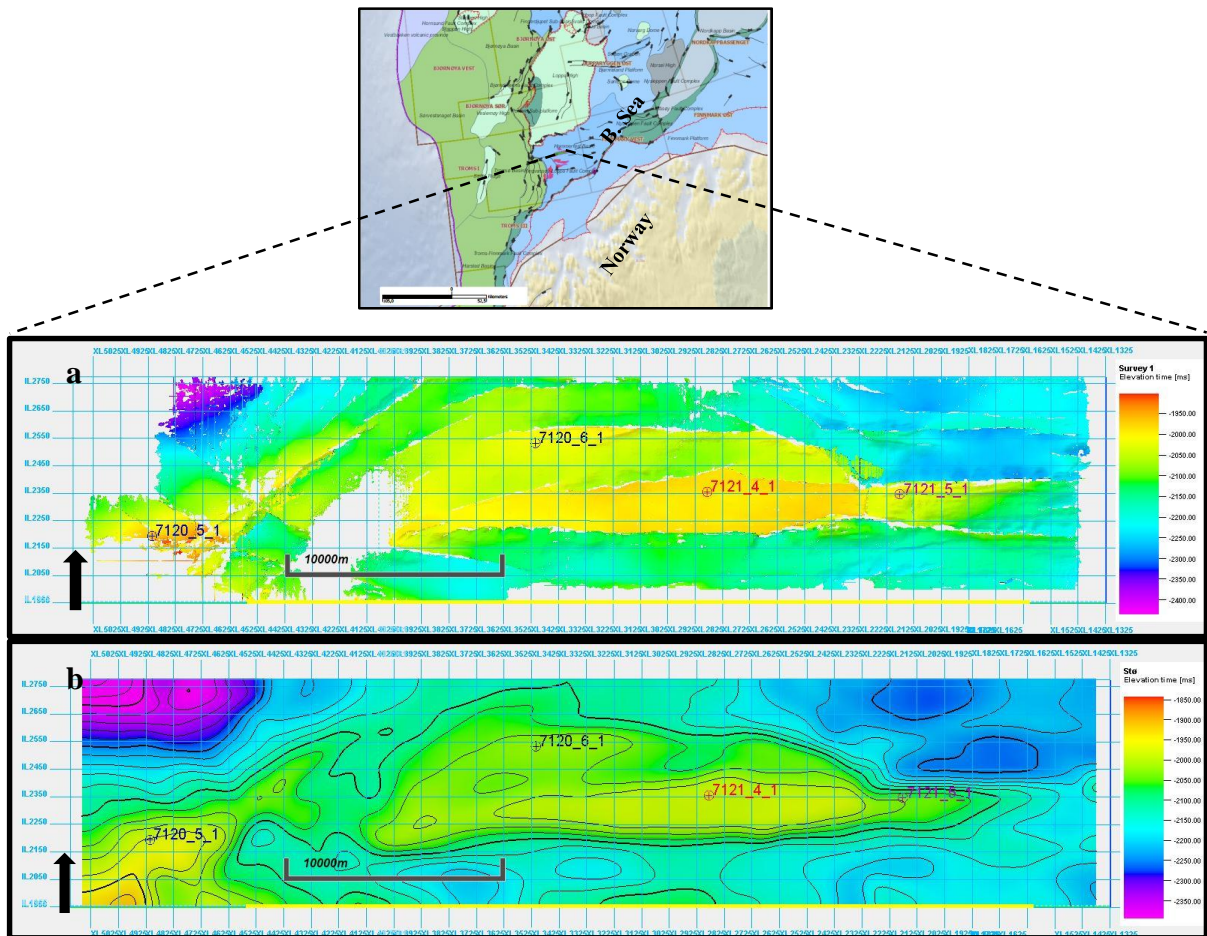


Figure 12: The Top Stø Surface; **a** Seeding 3D Auto-tracking and **b** the corresponding smoothed surface.

5.1.3 The Top Nordmela Formation

The Top Nordmela Formation has a lower acoustic impedance contrast almost in the whole cube and, as a result, lower reflectivity. Indeed, the confidence on mapping this horizon through *Seeding 3D Auto – Tracking* was poorer, see figure13 a.

Both *Seeding 3D Auto-tracking* surface (figure 13 a) and the corresponding smoothed surface (figure 13 b) resemble the same except for some minor area and areas where the data had been interpolated.

In the centre and on the south-western surface part there are the most elevated areas, on north-eastern exist two separated synclinal shape, on the north-western one sharp synclinal shape,

and on the south 3 smaller synclines shape. In fact, the violet colour is present in north-eastern and north-western, the deeper blue at the south and the green in the centre and south-eastern areas.

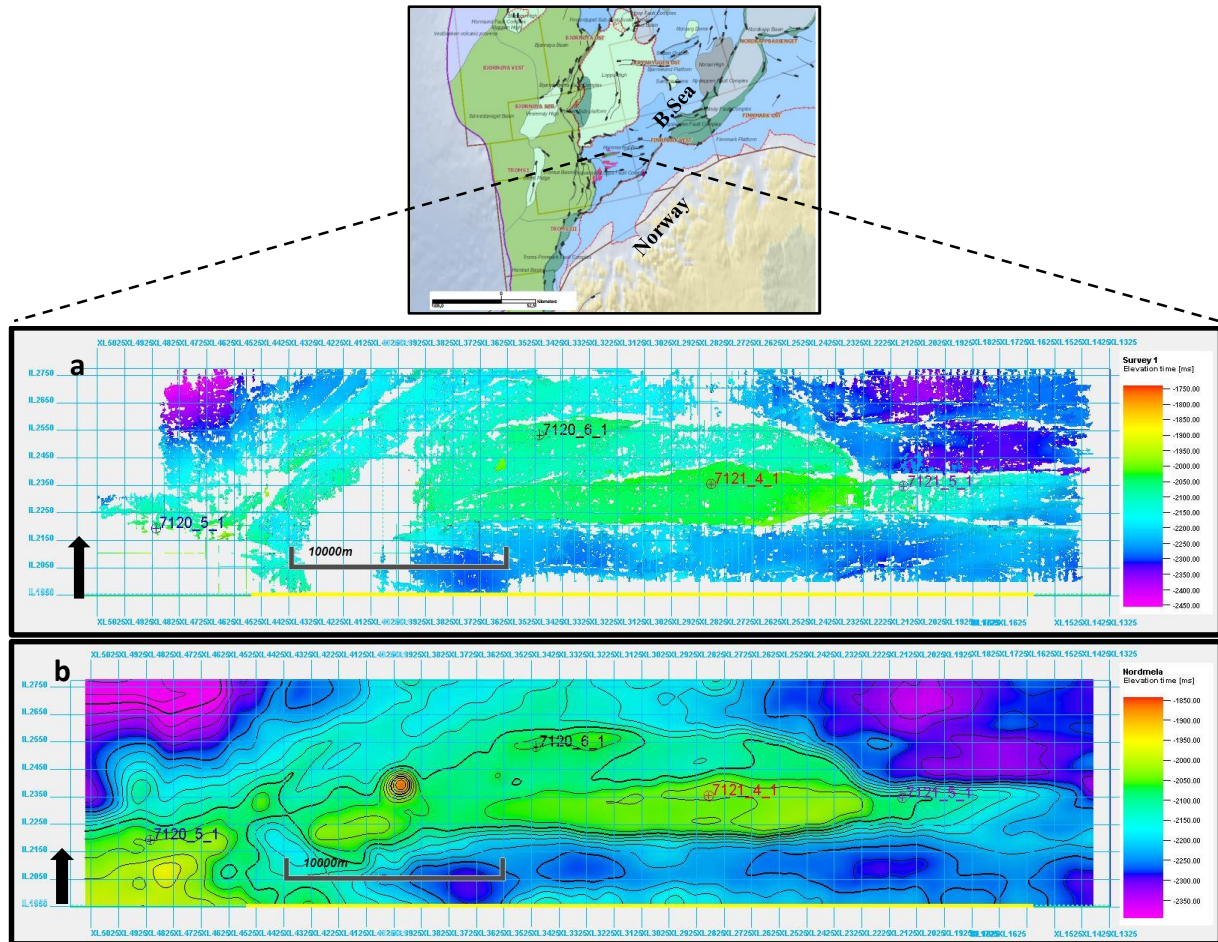


Figure 13: The Top Nordmela Surface; **a** Seeding 3D auto tracking and **b** the corresponding smoothed surface.

5.1.4 The Top Tubåen Formation

The Top Tubåen Formation has the lowest acoustic impedance contrast in the seismic scale almost in the entire cube and, as a result, lowest reflectivity. When mapping this horizon the confidence through *Seeding 3D Auto-Tracking* was poorer see figure 14 **a**.

Both Seeding 3D Auto-tracking surface (figure 14 **a**) and the corresponding smoothed surface (figure 14 **b**) show almost the same characteristic although the elevated area are not clearer separated on the figure 14 **a** and the deepest area on the south-eastern area do not exist on the figure 14 **b**. On the centre and south-western surface there are the most elevated surface areas,

whilst on north-eastern exist one synclinal shape and, on the north-western one sharp synclinal shape exist. The colours change sharply northward meaning existence of faults in opposite direction and separating the areas. However, on the north-eastern area the gradual blue colours change is related to the smooth synclinal and the change from light blue to violet is relate to sharp synclinal shape.

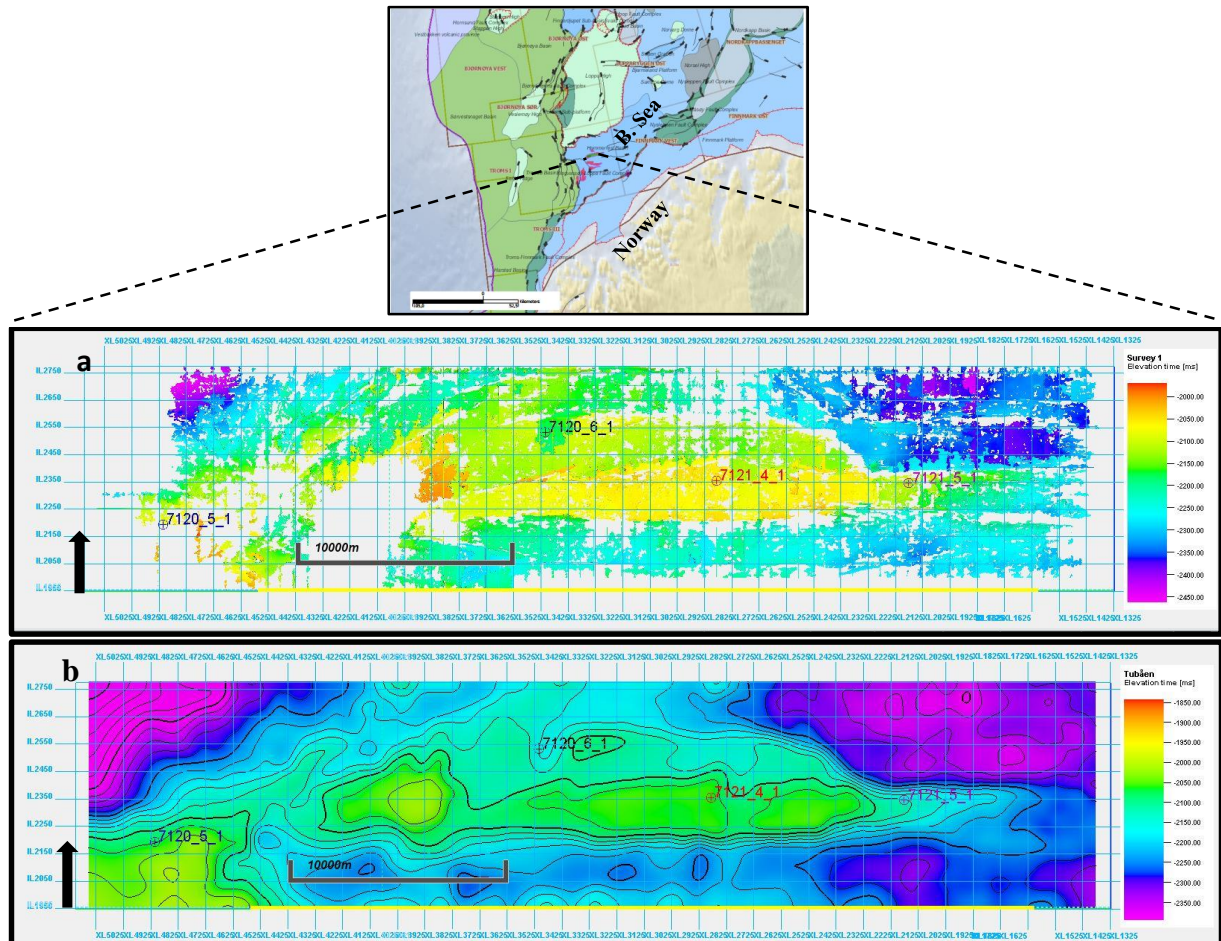


Figure 14: The Top Nordmela Surface; **a** Seeding 3D auto-tracking and **b** the corresponding smoothed surface.

5.2 Interpreted faults

The interpreted faults in the area are mainly dip-slip normal faults. However, listric normal faults have also been encountered in some small areas where was seen blocks rotation.

Taking into account the faults orientation, in this work two basic families of faults are recognized; the interpreted faults assigned indices A and others assigned indices B respectively. The indices A faults are easily seen in the crosslines (south-north orientation). They correspond

to principal normal faults in the study area and minor faults which tend to be parallel to the previous.

These faults plane are mainly east-west oriented, parallel to the In-lines and, in most cases, one fault begin in a close end or even at the end of perpendicular plane of other faults.

These faults are F 1A, F 2A, F 3A, F 4A, F 5A, and F 6A which can be seen on the figure 15.

By contrast, the other family of faults are commonly and easily seen in the In-lines and correspond to the minor faults with different orientation from the previous. These faults include minor faults spread all over the cube. They have mainly NW–SE and NE–SW orientation, therefore, these represent antithetic faults. These faults were named F 1B, F 2B, F 3B, F 4B, F 5B, F 6B, F 7B, F 8B F 9B and F 10B.

The Fault F1B intersect the principal fault F6A and the Fault F10B intersect the principal fault F 4A.

Although not clearly displayed, and based on the direction of the interpreted faults the area affected by a gas chimney may be crossed by faults F 6A, F 1B and F 4B.

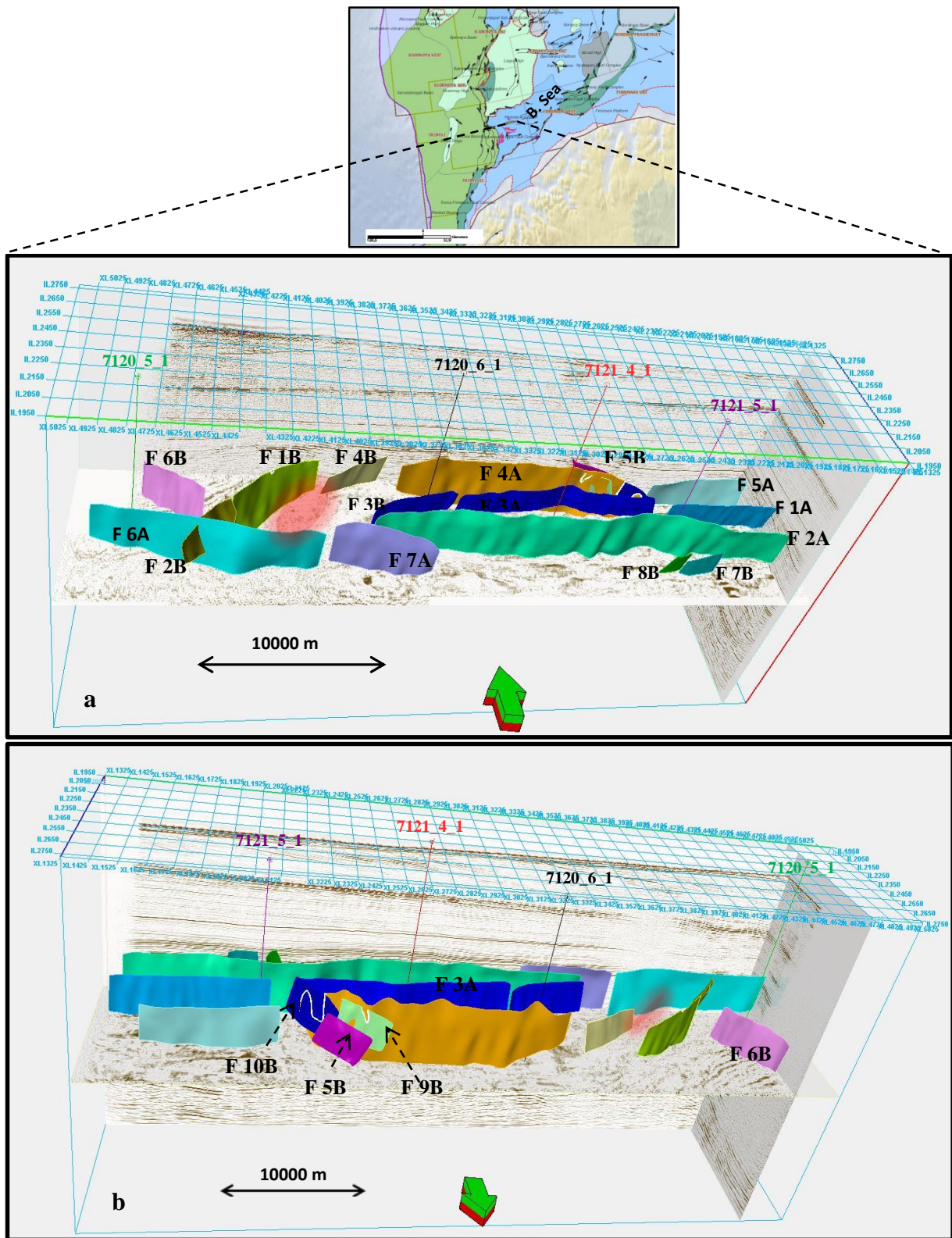


Figure 15: The normal principal faults, assigned indices A and antithetic faults assigned indices B and the *Gas Chimney* area in red inside the cube.

5.3 Reservoir signature

The area of interest in reservoir area is in the intervals between the Top Hekkingen Formation and the base of Nordmela. Based on the wells logs trend the general reservoir information is written;

The Sonic Logs have a decreasing trend in all the wells while the Gama Ray Log has an upward trend until it reaches the top Flugen Formation. From there it experiences variations;

Immediately above the Flugen Formation, in the Lower Hekkingen Formation the Gamma ray is high and it decreases with depth, having the slowest value in the lower part of the Stø Formation.

The area in yellow designated “X over” resulted from insertion of the Density and Neutron logs in the same track being the Neutrons scale inverted, is present within the Stø and part of Nordmela Formation.

However, non-similarities may be observed; the separation between the resistivity logs, the “X over” as well as the logs values differ from one well to other.

The Gamma Ray log in Hekkingen Formation shows high values (more than 120 gAPI), going out of the scale in in the entire wells. Its high value may be associated with the shale presence in the Hekkingen Formation.

Below, in the Stø Formation there is minimum Gamma Ray value relative to entire wells. In this interval, the resistivity is high (excepting for well 7121_6_1), the Density log is sitting at the right side relative to the Neutron logs; these are typical the characteristics of the reservoir. Integrating the logs in this area with additional well information this may be interpreted as sandstone containing hydrocarbon. The sandstone in same interval contains a small quantity of shale.

In some wells this trend continues to the next Formation, the Nordmela Formation, although the good trend relative to good reservoir can be hardly seen. Due to the fact that the Gamma Ray increases compared to previous good reservoir and associating the well information, it may be said that the siltstone in the Nordmela Formation may have shale embedded which increases the Gama Ray value.

Below in the figure 16 is displayed the composite log in the reservoir area for one well. The individual logs may be encountered in the appendix. Note that the well tops Formations have been flattened on the Stø Formation.

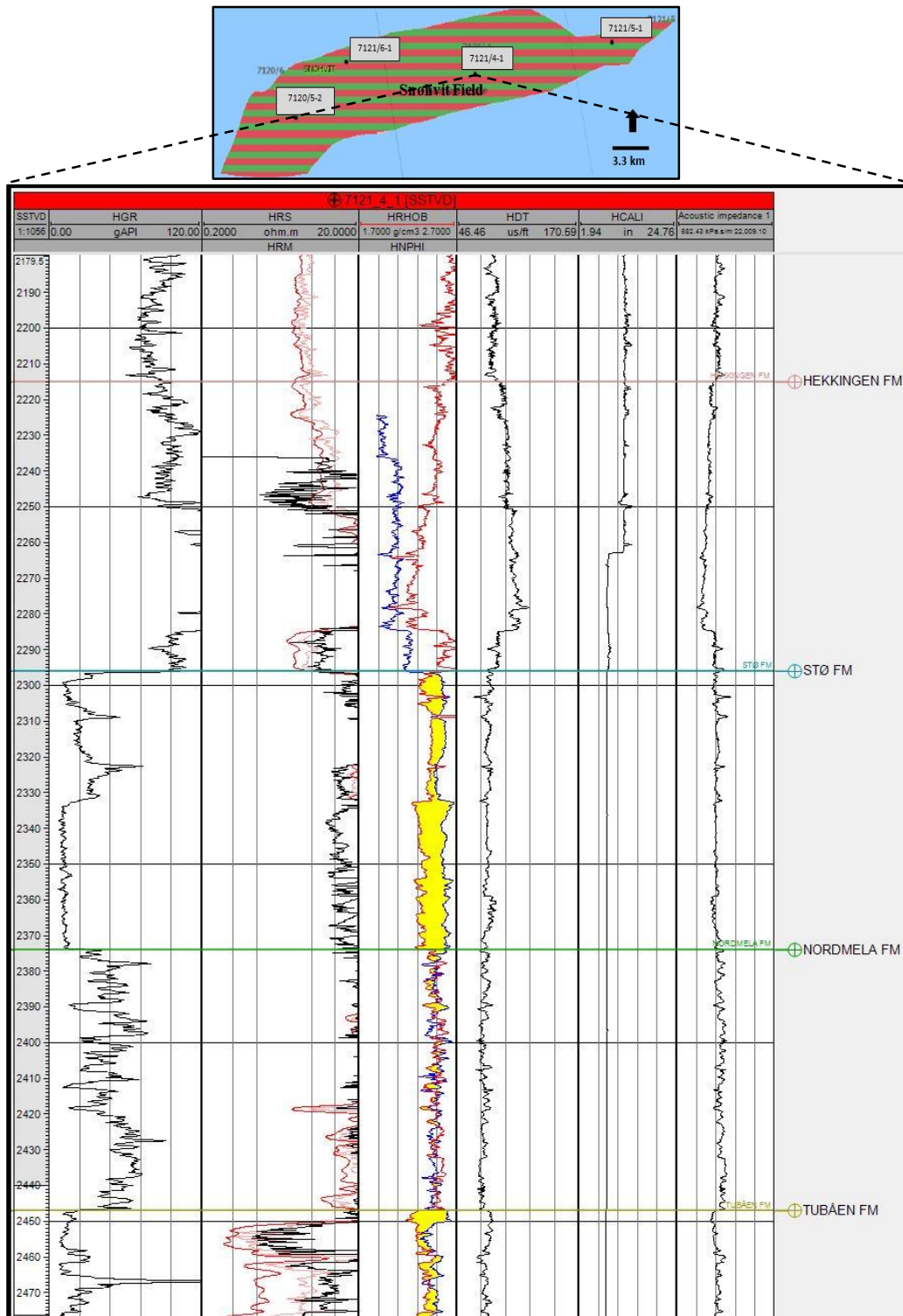


Figure 16: The reservoir signature in the Snøhvit Field for well 7120_4_1. In the second track the deep blue, light and black colours represent respectively deep, medium shallow resistivity.

5.3.1 Gas-Oil and Oil-Water Contacts in the reservoir

The fluid contacts in the reservoir can be visualized through seismic data, however, it happens that not all the seismic data in the reservoir display this hydrocarbon indicator. In such case, as in this particular case, one may rely on other data to locate this feature.

To determine the Gas-Oil and Oil-Water Contacts well data was used. Mainly the determination relied on Resistivity, Slowness and Density logs in the previous located reservoirs interval.

The oil and water have approximately the same density which makes difficult the use of density log to locate the separation between these fluids. However, in the three wells, namely 7120_6_1, 7121_4_1 and 7121_5_1 the fluid separation have been determined.

The well 7120_5_1 is not used in this type of studies as it contains a small amount of the hydrocarbon and therefore considered negative well.

The table below shows the interpreted fluid contacts coordinates (depth for well and time for seismic) for the three wells in the Snøhvit.

Table 2: The fluid contacts for both well and seismic data

Well	GOC	OWC
7121_4_1	2353 (m)	2375 (m)
	2038 (ms)	2061 (ms)
7121_5_1	2383.48 (m)	2410.37 (m)
	2093.33 (ms)	2099.93 (ms)
7120_6_1	2396.08 (m)	2420.3 (m)
	2074.4 (ms)	2081.57 (ms)

Fluid contacts in the Well 7121_4_1 and seismic Cube

In the reservoir interval the resistivity is high, as expected, being higher for the gas interval. The separation between Neutron Porosity (HNPHI) and Density (ROBH) logs in track 4 is overall less for gas zone than for oil and water zones. This track 4 can hardly be used for Oil-Water Contacts location. However, it turns out that water has lower resistivity and therefore should be easier to see this separation through resistivity logs. Still, other effects contribute negatively for this determination.

The interpretation of fluid contacts on the seismic cube has only been made inside the area of interest, which is in this case, the horst in between faults. Note that the area has been interpreted as one of the three different structures in the cube containing hydrocarbon. Both GOC and OWC are not regular surfaces.

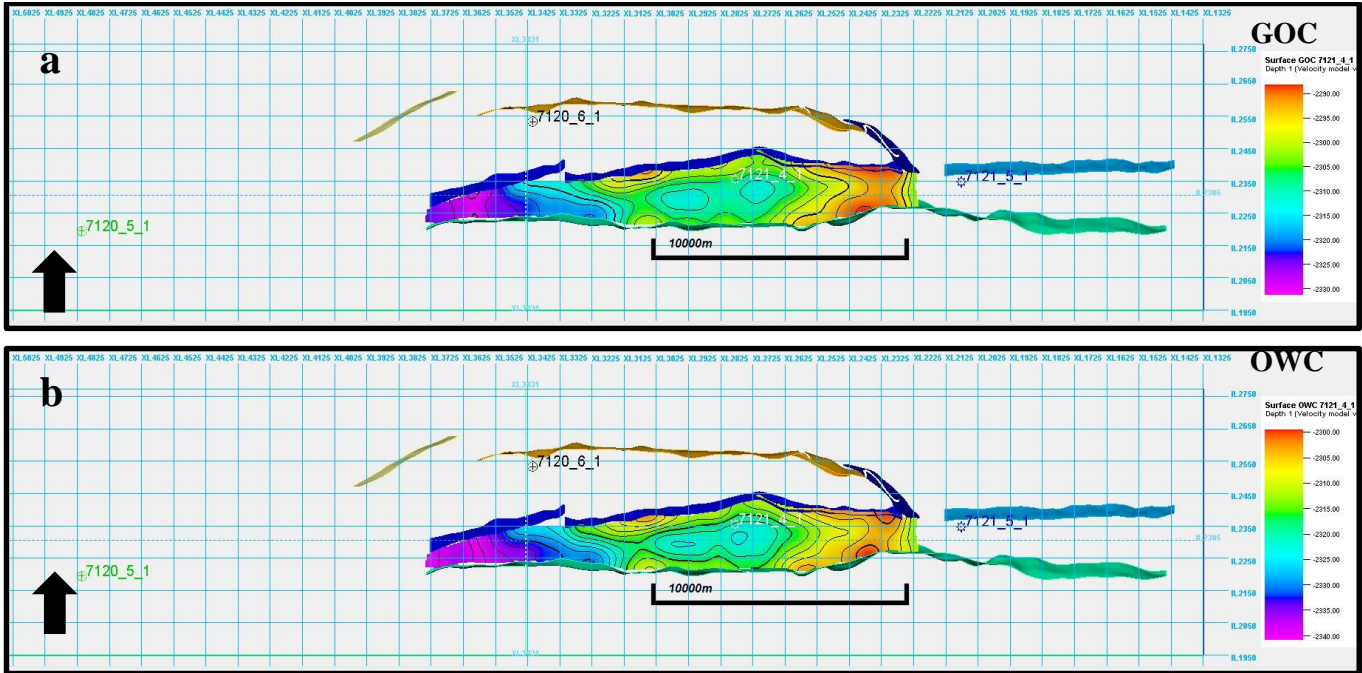


Figure 18: The irregular fluid contacts surfaces (a-GOC and b-OWC) in the horst area limited by faults inside the 3D seismic cube.

Fluid contacts in the Well 7121_5_1 and the seismic Cube

The resistivity is higher for gas interval than oil and water interval and, the track 4 shows similar behaviour compared to the previous well. Here, the water interval has not as lower resistivity as expected; the local resistivity characteristics may be influenced by other lithology factors. Still, it’s possible to point out the Oil-Water Contact.

Note that the Tubåen Formation also contain small amount of gas but due to increase in shale content, seen using gamma ray log, and tightness, confirmed by core data, this is not good reservoir, therefore, this intervals have been ignored.

The Gas-Oil Contact (GOC) was located in the 2383.48 meters depth in the composite logs corresponding 2093.33 mili-seconds in time through seismic section. On the other hand, the Oil-Water Contact has been determined in the coordinates 2410.37 meter and 2099.93 mili-seconds, both for well and seismic data. This correspondence was made based on the Time Depth Relationship (TDR).

The figure below shows fluids contacts in the reservoir interval in the well. It is clearer seen that the oil column is thinner than the Gas thickness.

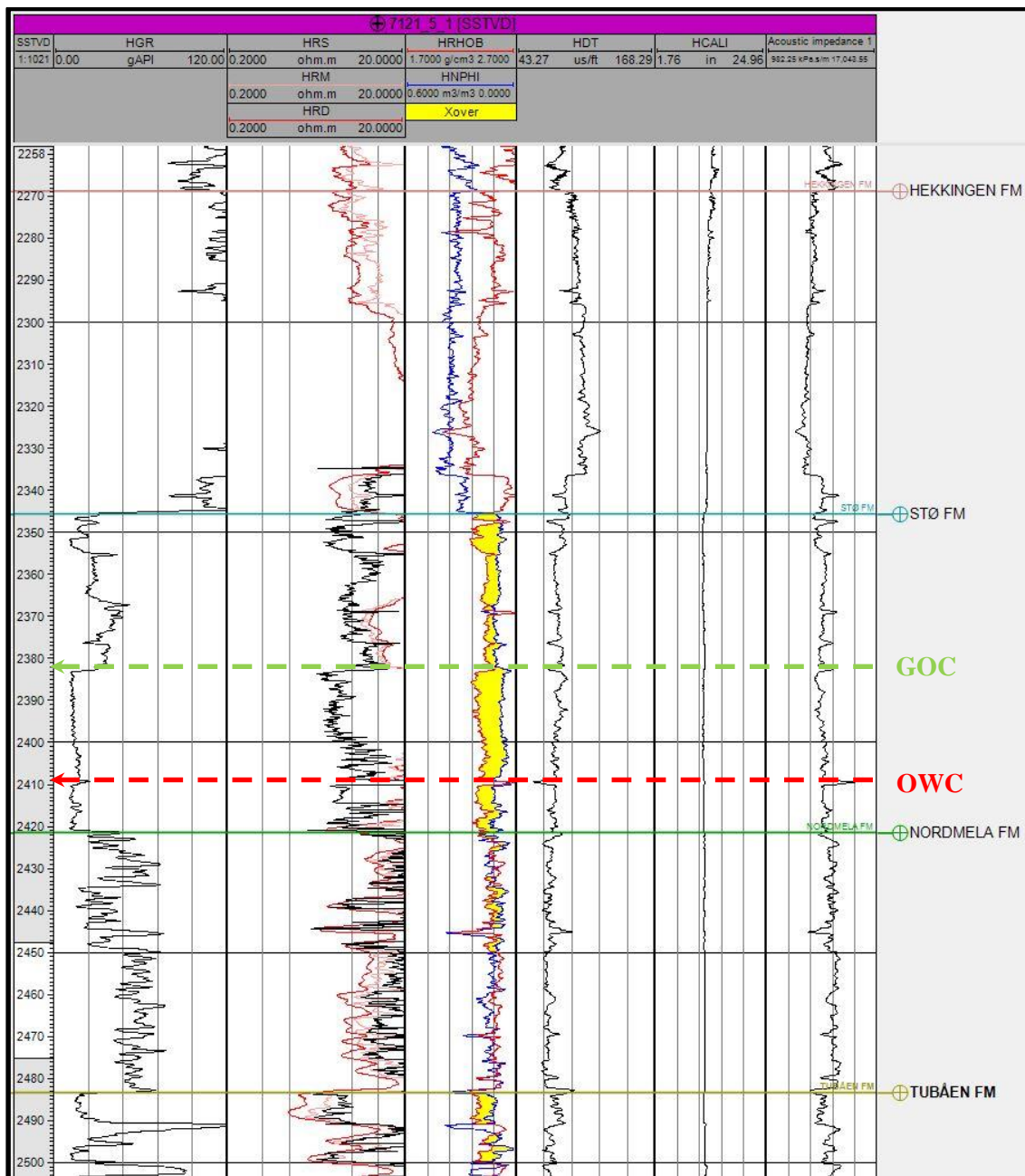


Figure 19: The interpreted oil and water contacts in the well 7121_5_1. The top gas is the Top Stø Formation

The fluid contacts have separately interpreted on the eastern rotated block, which is between the faults shown in seismic cube below. However, this structure does not separate from the previous by any interpreted faults.

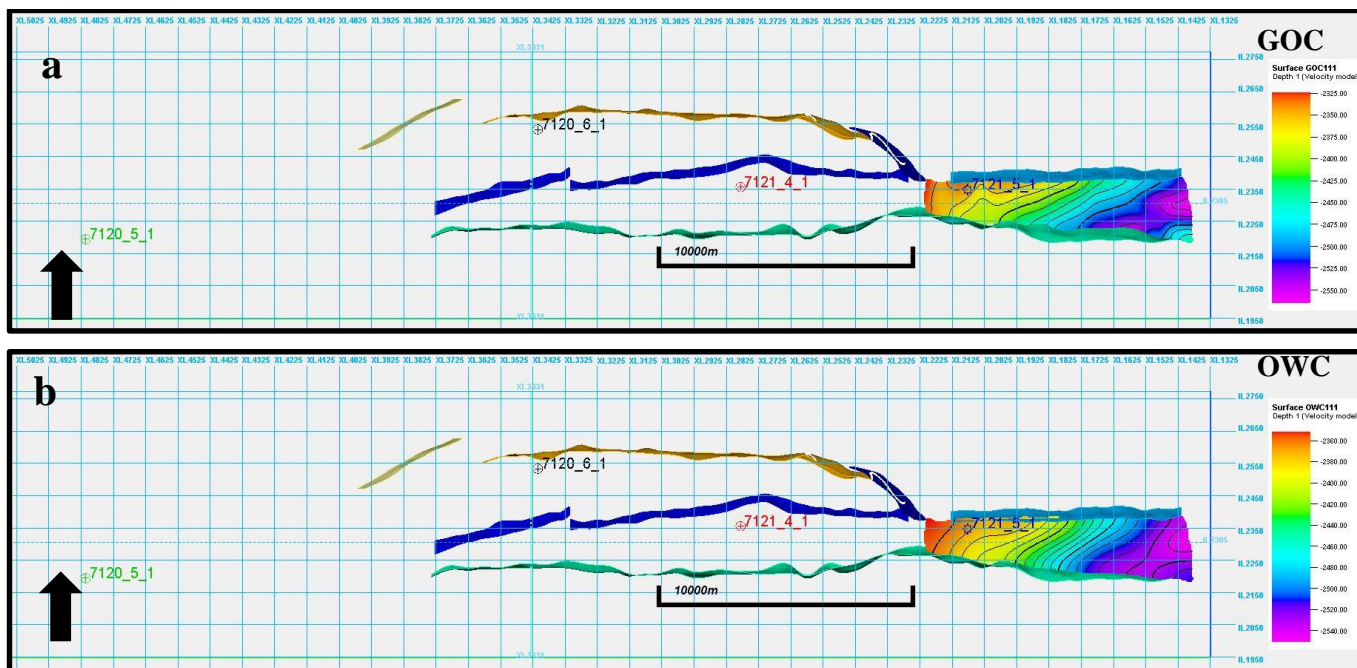


Figure 20: The irregular fluid contacts surfaces (a-GOC and b-OWC) in the rotated block limited by faults inside the 3D seismic cube.

Fluid contacts in the Well 7120_6_1 and seismic Cube

The resistivity is higher for gas interval than oil and water interval and, the track 4 shows similar behaviour compared to the previous wells. Here, the water interval has lower resistivity and easy to use for encountering the oil water separation signal in the well data.

Note that Nordmela and Tubåen Formations also contain small amount of gas but due to increase in shale content, seen by gamma ray log, and tightness, confirmed by core data, the good reservoir characteristics deteriorates, therefore, this intervals have been ignored.

The Gas-Oil Contact (GOC) was located in the 2426.08 meters depth in the composite logs corresponding 2074.4 mili-seconds in time through seismic section. The Oil-Water Contacts have been determined in the coordinates 2442.3 meter and 2081.57 mili-seconds, both for well and seismic data. This correspondence was made based on the time depth relationship (TDR).

The figure shows fluids contacts in the reservoir interval in the area crossed by the well. It is clearer seen that the oil column is thinner than the gas thickness.

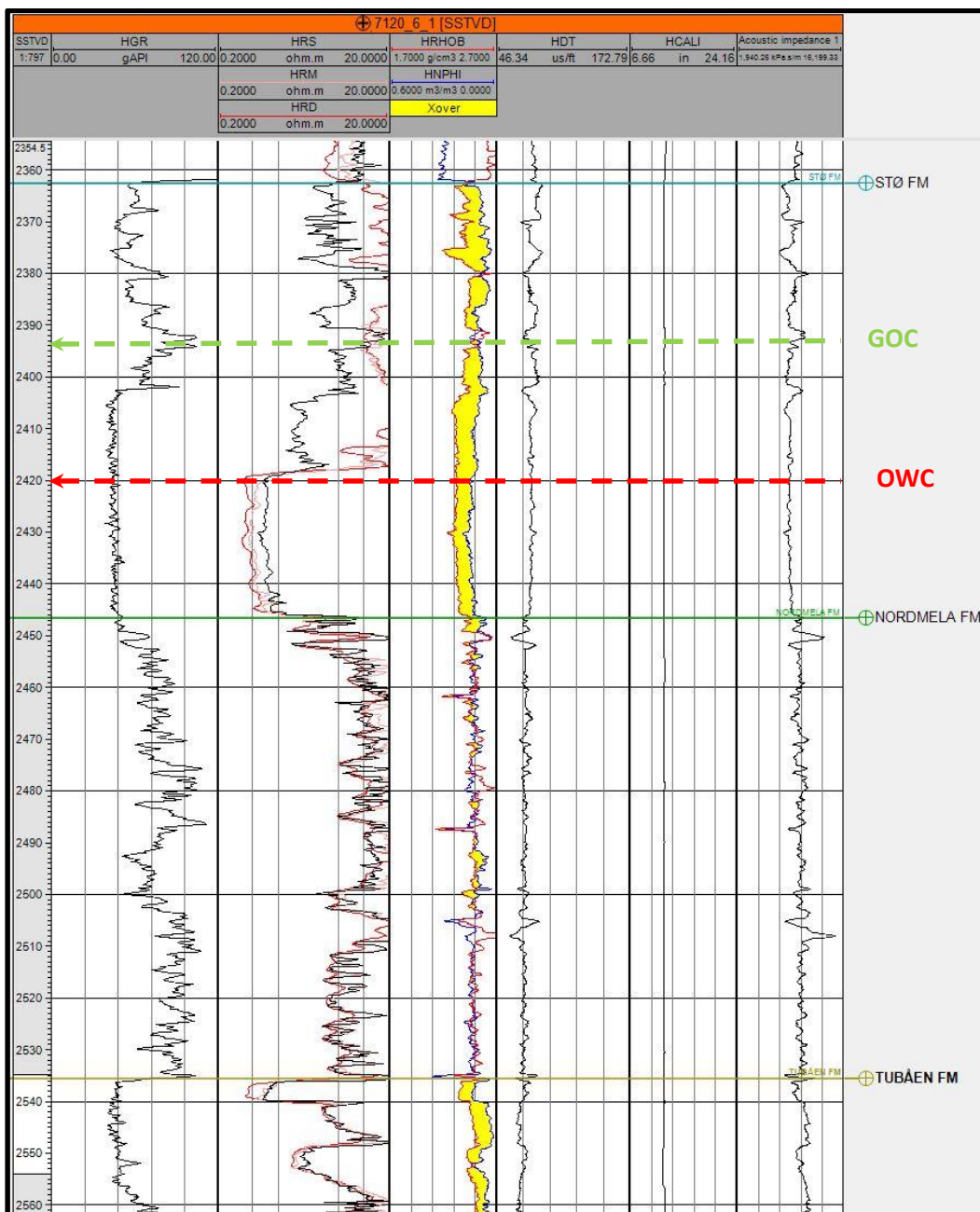


Figure 21: The interpreted oil and water contacts in the well 7121_6_1. The top gas is the Top Stø Formation.

The interpretation of fluid contacts in the seismic data has only been made inside the area of interest which is, in this case, into the graben.

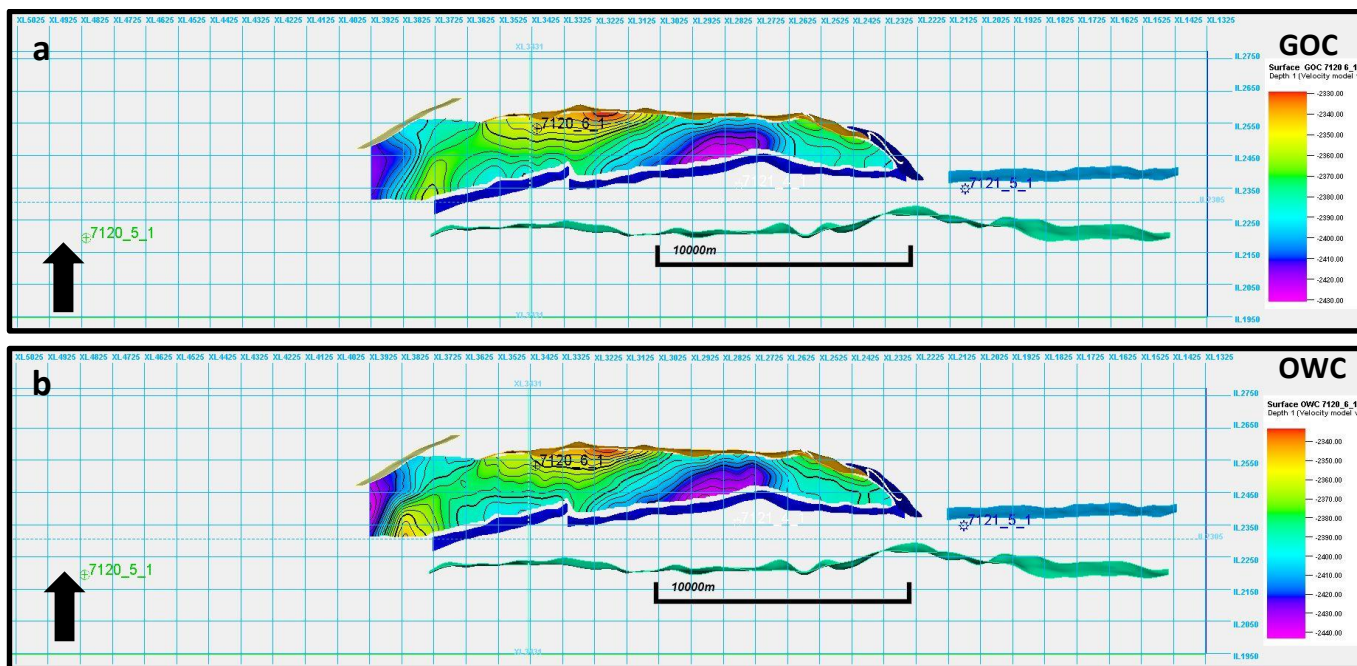


Figure 22: The irregular fluid contacts surfaces (a-GOC and b-OWC) in the graben limited by faults inside the 3D seismic cube.

5.4 Velocity Model in the reservoir interval

On Petrel Software it is possible to visualise data which are in different domain, i.e., time and depth domain. However, when integrating this data for particular studies one should work in one domain. Therefore, to convert objects (surfaces, horizons, points, etc.) from one domain to other (time to depth or vice versa) a velocity model has to be built. It can be built using well data which includes the calibrated sonic, well tops data and average velocity from Time Depth Relation (TDR). Note that only objects converted by the same velocity model can be displayed together. (Schlumberger, 2014)

Defining the intervals velocity taking as input the smoothed surface and the average velocity, and inserting the average velocity taken from Time Depth Relationship, in this study a velocity model was defined. Thereafter, conversion of the surfaces including the fluid contacts took place from time to depth domain as the main goal is to work on depth domain.

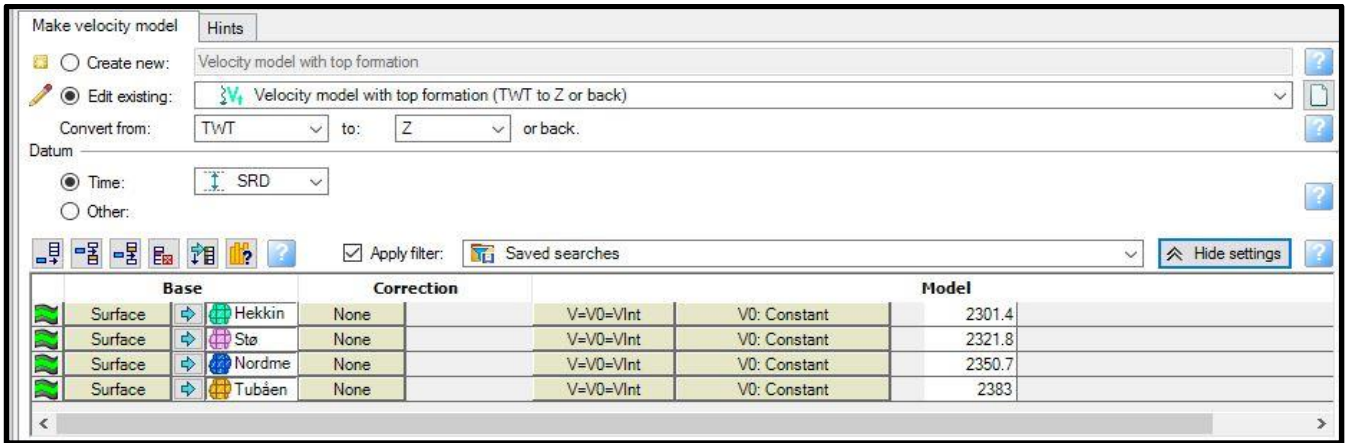


Figure 23: The input on the built simple velocity model.

6. Discussion

In a seismic scale and using zero phase seismic data, the Tubåen Top Formation was interpreted as through while the others Top Formations had been interpreted as peaks see figure 24. However, in a more detailed scale, every one meter (on wells), this is not obvious for all the Top Formations well. Actually, in the well 7121_4_1 the acoustic impedance reduces through Hekkingen and Tubåen Formations tops suggesting low horizons reflectivity, and, spikes in the acoustic impedance are observable for Stø and Nordmela Formation. Therefore, the suggesting reservoir signature through the seismic scale does not agree with a reservoir signature locally seen in the well 7121_4_1 except for Tubåen Top Formation.

The area containing *Gas Chimney* see figure 15 a may be crossed by faults if one takes into consideration their orientation. As a result, the surfaces dip, or colour change in this area should be easily seen in the cube. This does not happen probably because the resulted surface had taken only the Seeding 3D Auto - tracking surface as input living behind the faults orientation.

Although in areas all over the cube the interpreted seismic reflector agree with the well Formation tops, in the well 7120_5_1 there is a mis-tie. This was due to poorer tie as was realized later on when building velocity model for converting data into depth domain. Therefore, the area in violet colour is not has precise as it should be.

Some faults F 1B, F 2B, F 2A and F2B seems to be the same fault in a large scale, however, if it is seen in detail they have a slight different orientation and/or the fault beginning plane does not coincides with the end of others, therefore these have been interpreted as a different faults.

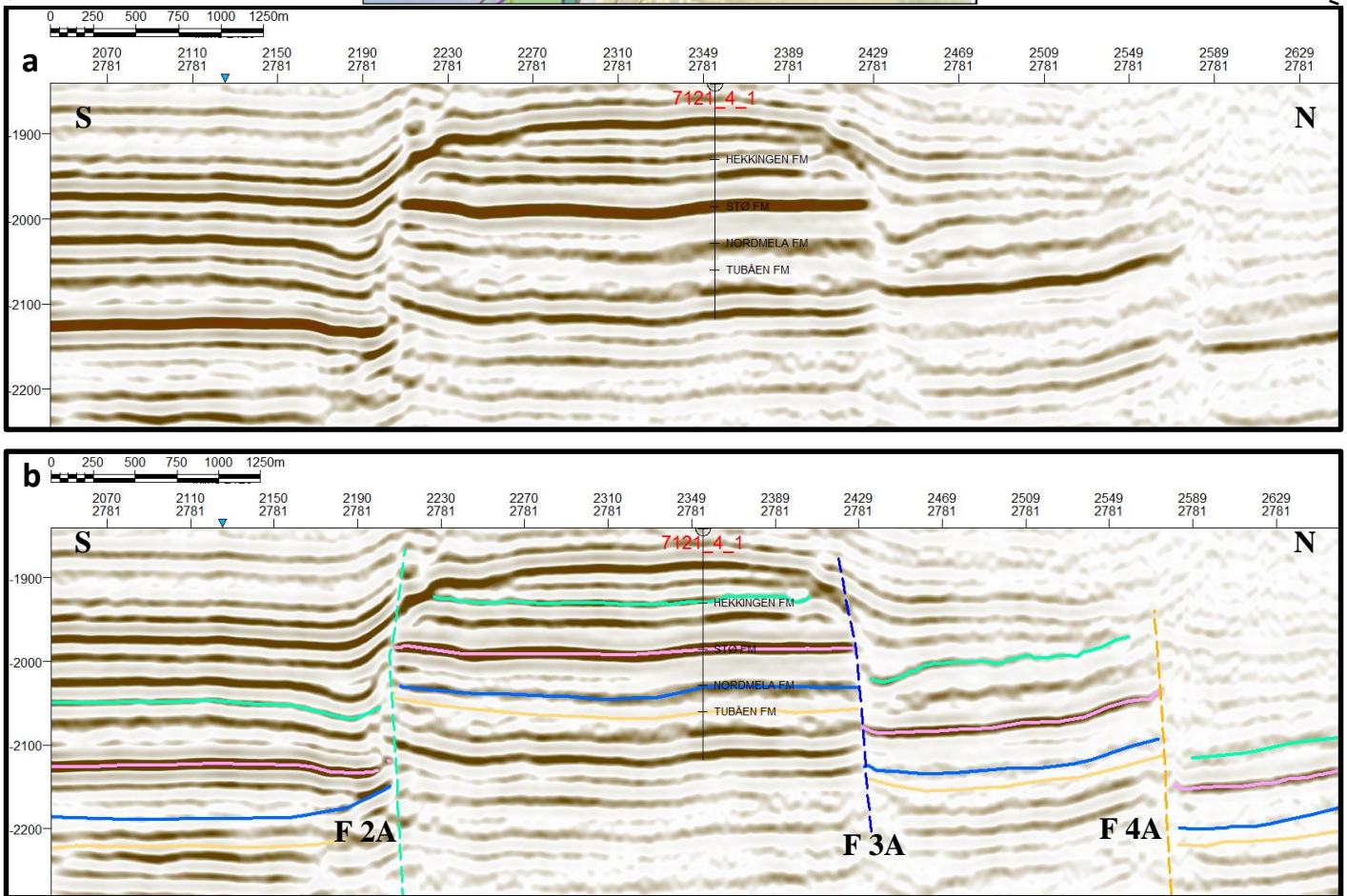
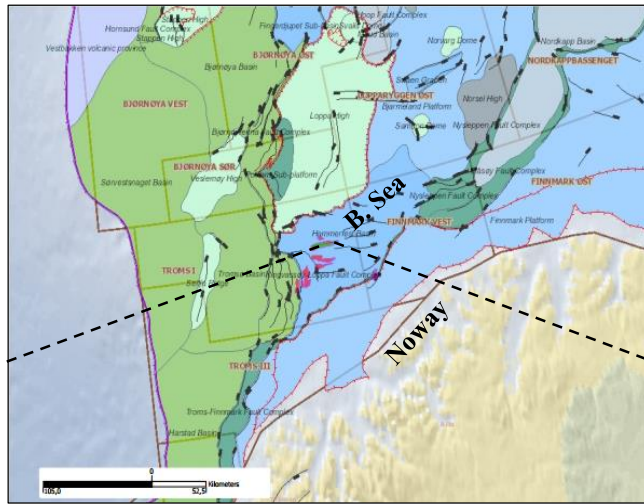


Figure 24: The four interpreted horizons in the Snøhvit field. All have been interpreted as a peak except the Tubåen Formation.

7. Conclusion

The seismic data is valuable in both geology and geophysics. It can be integrated with other different data with the goal to build and improve subsurface model, and thereafter, plan strategies for better resources exploration.

Using Snøhvit 3D seismic and well data integrated into Petrel® 2015 the following has been concluded;

- The faults in the reservoir and nearer Formations are dip slips normal and minor listric faults.
- The main faults are oriented west-east direction whist antithetic, minor faults, mainly are oriented SW – NE and SE-NW, see figure 15,
- The ovals gas chimney shape are in the west of the cube has the same orientation to certain minor antithetic faults and might be crossed by more fault (in addition to F 6A, F1B and F4B), however, due to dimming effect the area was not mapped, see figure 10 and figure 15 **a** and 15 **b**.
- The reservoir and nearer Formations were severe faulted and the horizons laterally segmented, see figure 15 **a**, 15 **b** 17 **a** and 17 **b** and 24;
- The tops surfaces Formations dip sharply to north-western and north-eastern at the end of the cube, and, by contrast, dip gently on the western direction as can be seen on figures 11 up to 14.
- The fluid contacts are in different level for the three interpreted structures inside the cube, suggesting no communication within the structures, see figure A 13 in the appendix

8. Reference

- ALVES, T. M., OMOSANYA, K. D. & GOWLING, P. 2015. Volume rendering of enigmatic high-amplitude anomalies in southeast Brazil: A workflow to distinguish lithologic features from fluid accumulations. *Interpretation*, 3, A1-A14.
- BIGELOW 1995. Introduction to wireline Log analysis. Western atlas international Houston, Texas 326.
- BROWN, A.R.2004. Interpretational of three dimensional seismic data. Tulsa, American association of Petroleum Geologists. Volume 42.
- CLARK, S. A., GLORSTAD-CLARK, E., FALEIDE, J. I., SCHMID, D., HARTZ, E. H. & FJELDSKAAR, W. 2014. Southwest Barents Sea rift basin evolution: comparing results from backstripping and time-forward modelling. *Basin Research*, 26, 550-566.
- FALEIDE, J. I., GUDLAUGSSON, S. T. & JACQUART, G. 1984. Evolution of the western Barents Sea. *Marine and Petroleum Geology*, 1, 123-150.
- GABRIELSEN, R. H., FAERSETH, R. B. & JENSEN, L. N. 1990. Structural Elements of the Norwegian Continental Shelf. Pt. 1. The Barents Sea Region, Norwegian Petroleum Directorate.
- KEAREY P. Brooks M. Kearey P. & Hill A. 2002. An Introduction to Geophysical Exploration. Blackwell Science Ltd, Oxford. Third Edition
- LARSEN, B. T. O., SNORRE ; BJORN, SUNDEVOLL AND MICHEL HUREMANS 2005. Volcanoes and Faulting in an arid climate. In: RANGNES, I. B. R. I. B. A. N. K. (ed.) *The making of a Land ; Geology of Norway*. Norway: Geological Society Publishing House.
- LINJORDET, A. & OLSEN, R. G. 1992. The Jurassic Snohvit Gas Field, Hammerfest Basin, Offshore Northern Norway: Chapter 22.
- LOWRIE W. 2007. Fundamentals of Geophysics. Cambridge University Press, Cambridge. Second Edition
- MILSON J. 2003. Field Geophysics: The Geological Field Guide Series. John Wiley and Sons Ltd, England. Third Edition
- REYNOLDS J. M. 2007. An Introduction to Applied and Environmental Geophysics. John Wiley and Sons Ltd, England.
- RITZMANN, O. & FALEIDE, J. I. 2007. Caledonian basement of the western Barents Sea. *Tectonics*, 26, TC5014.
- RONNEVIK, H., BESKOW, B. & JACOBSEN, H. P. 1982. Structural and stratigraphic evolution of the Barents Sea.
- SCHLUMBERGER. 2014. Petrel Geophysics, Seismic Visualization an Interpretation.
- TALWANI, M. & ELDHOLM, O. 1977. Evolution of the Norwegian-Greenland sea. *Geological Society of America Bulletin*, 88, 969-999.
- ZIEGLER, P. A. 1978. North Sea Rift and Basin Development. In: RAMBERG, I. & NEUMANN, E.-R. (eds.) *Tectonics and Geophysics of Continental Rifts*. Springer Netherlands.

Appendix

The composite logs

The composite logs in four (4) wells and some well Top Formation inside the Snøhvit cube area. All the well Top Formation have been flattened on the Stø well Top Formation

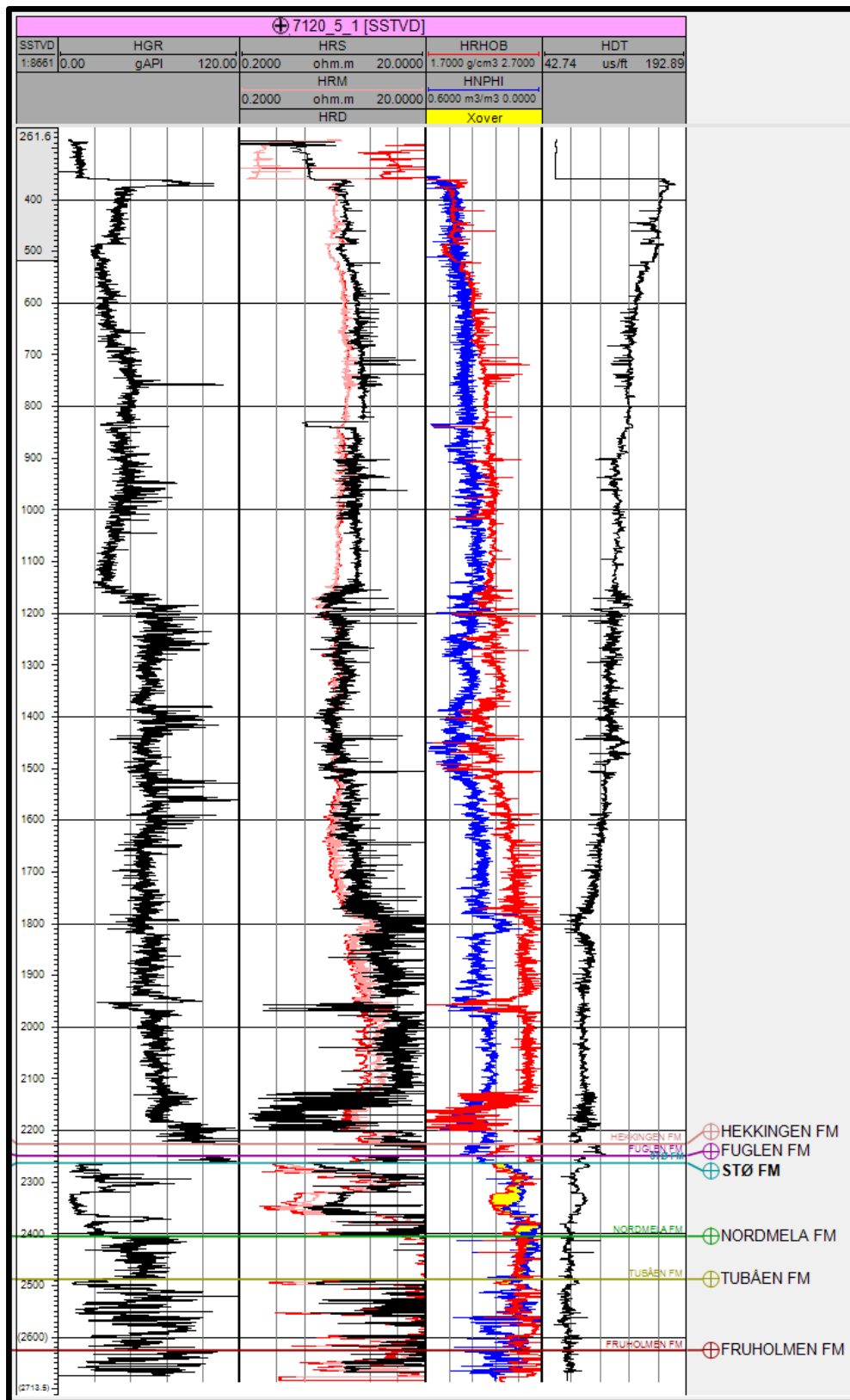


Figure A 1: The 7120_5_1 wells composite log in the Snøhvit field. The logs initiate at the 260 meters depth.

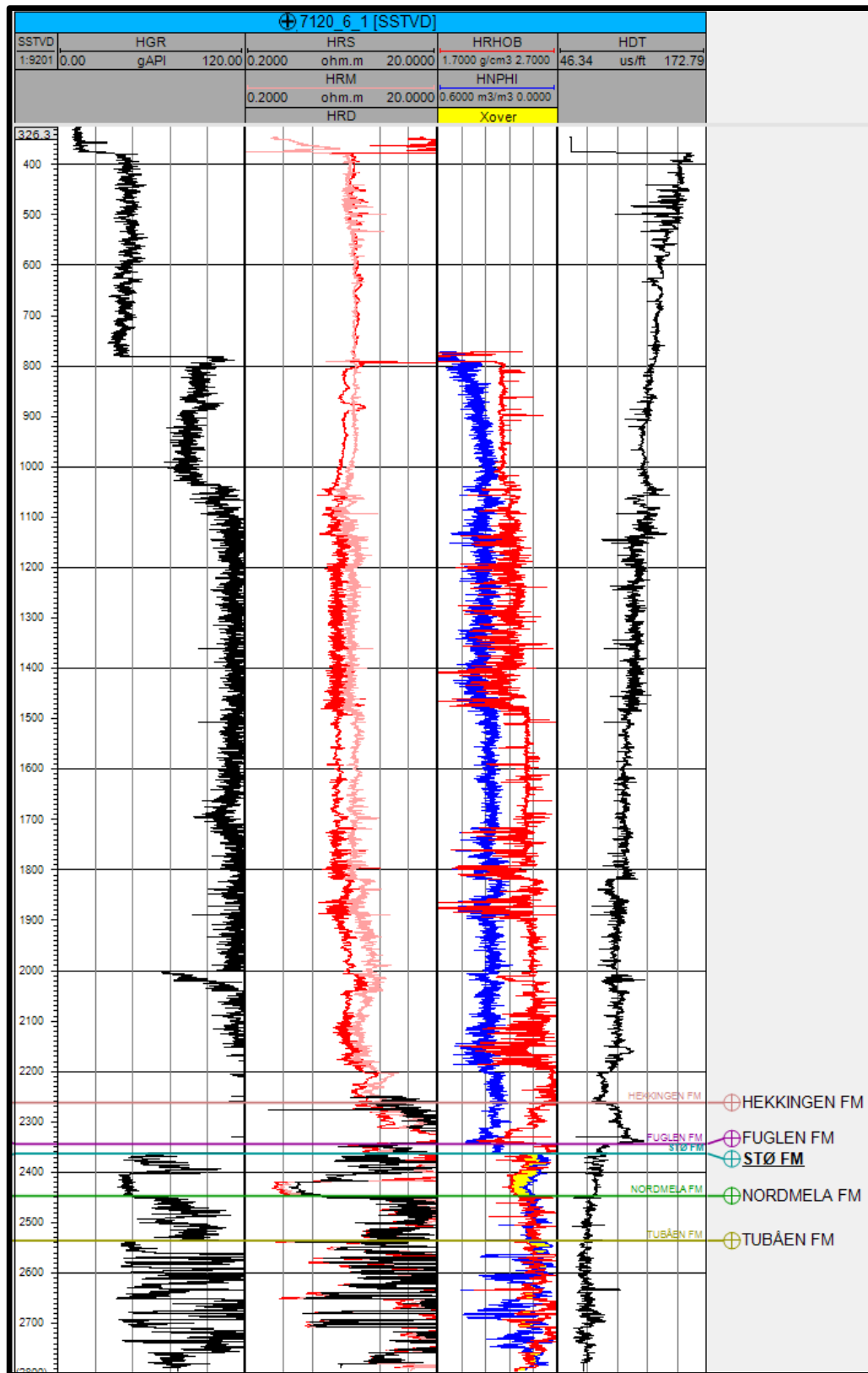


Figure A 2: The 71720_6_1 wells composite log in the Snøhvit area. The logs initiate at about 325 meters depth.

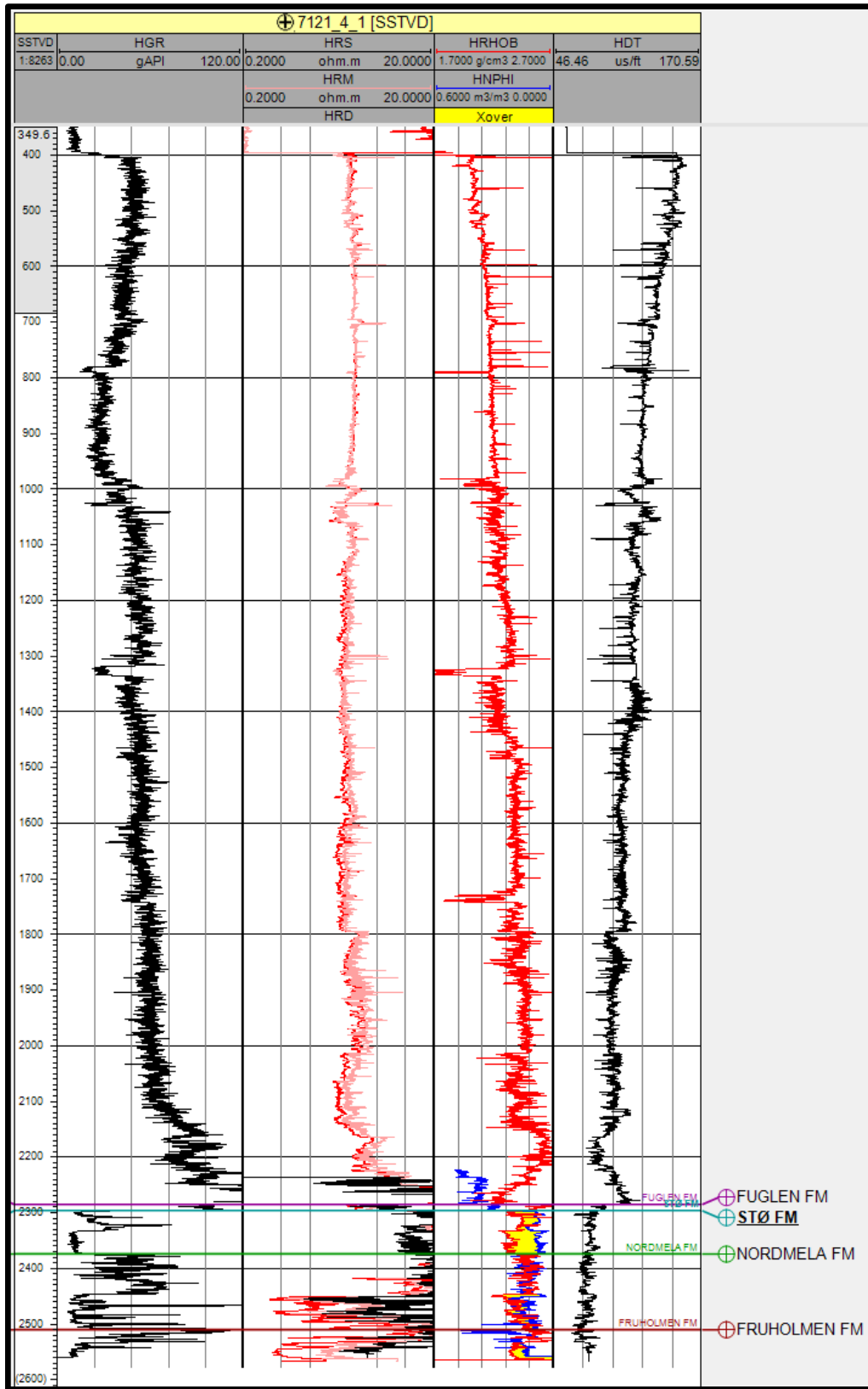


Figure A 3: The 7121_4_1 wells composite log in the Snøhvit area. The logs initiate at about 349 meters depth.

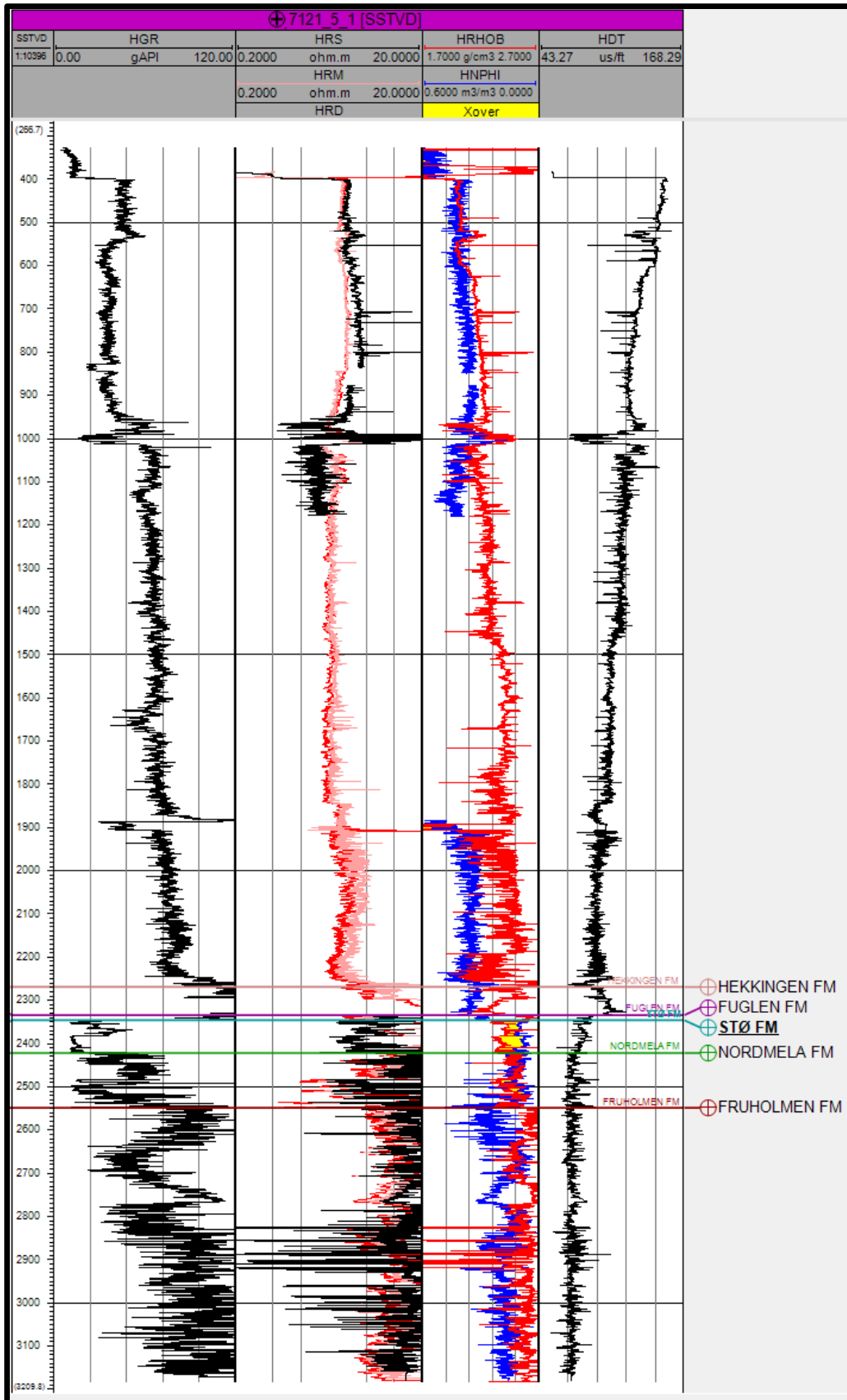


Figure A 4: The 7121_5_1 wells composite log in the Snøhvit area. The logs initiate at about 285 meters depth.

The composite logs in the reservoir area

The area of interest is the reservoir interval. Therefore the reservoir signature is shown in this area. Note that in addition to the previous logs, is displayed the acoustic impedance.

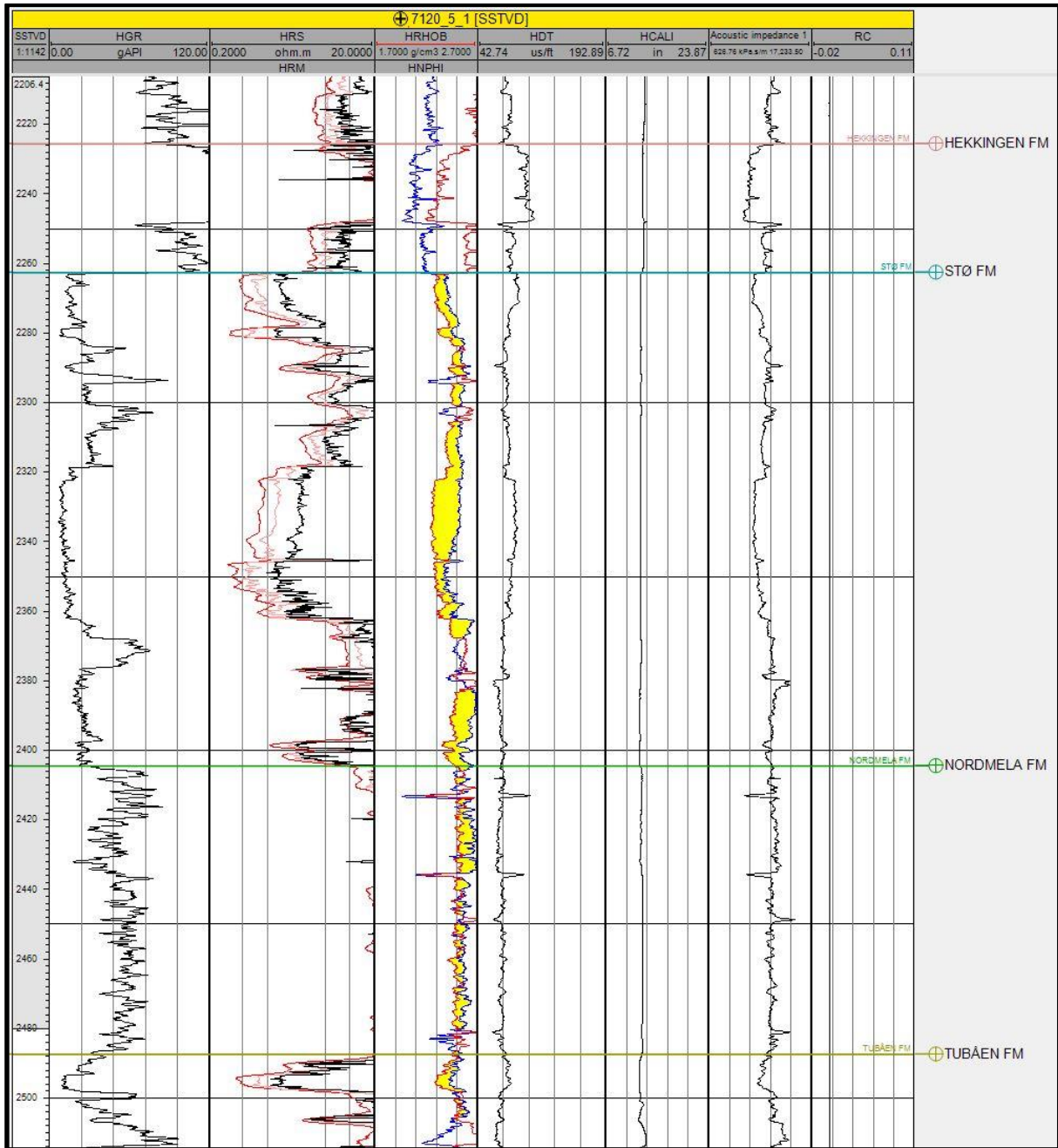


Figure A 5: The composite log in the reservoir interval for the well 7120_5_1.

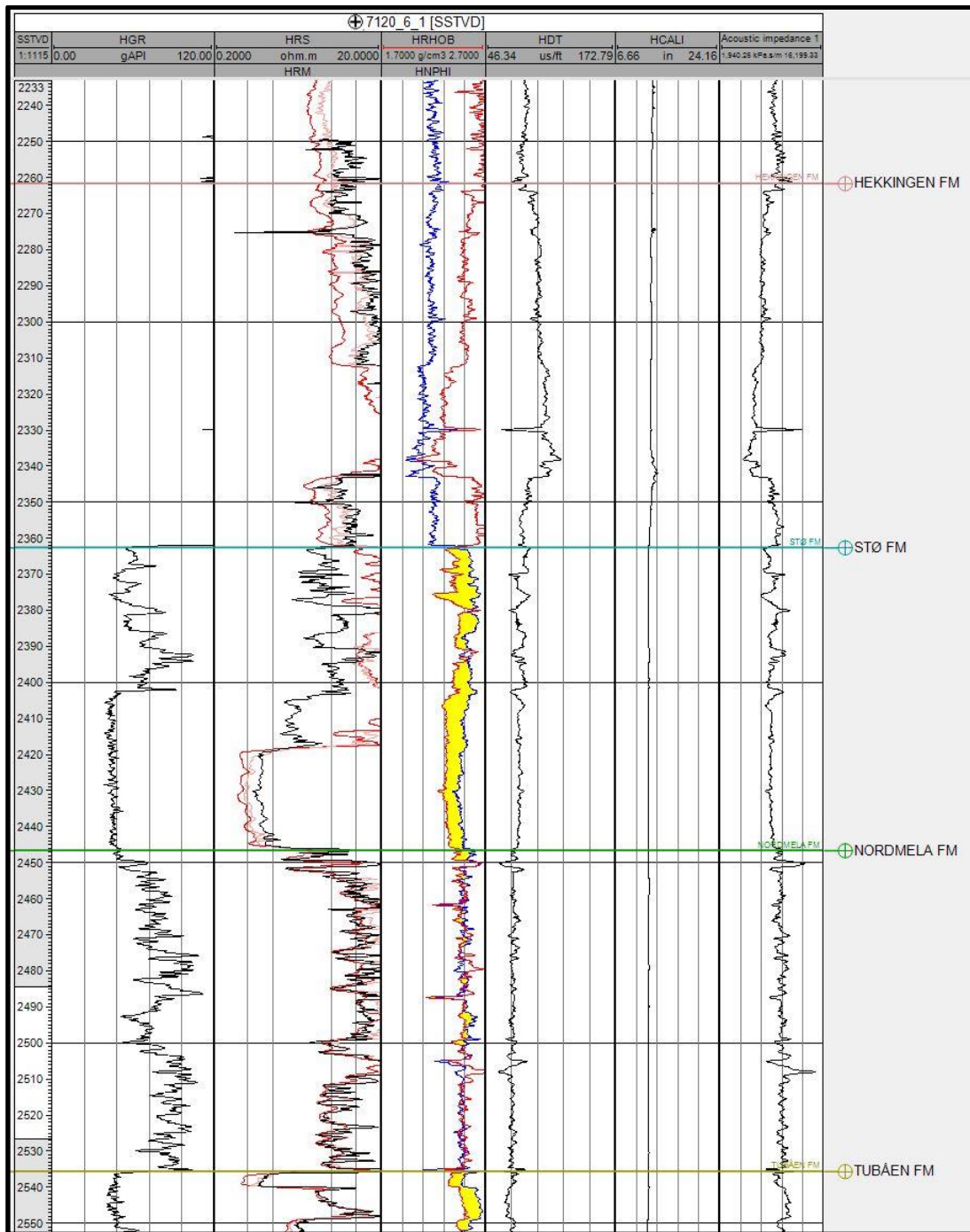


Figure A 6: The composite log in the reservoir interval for the well 7120_6_1.

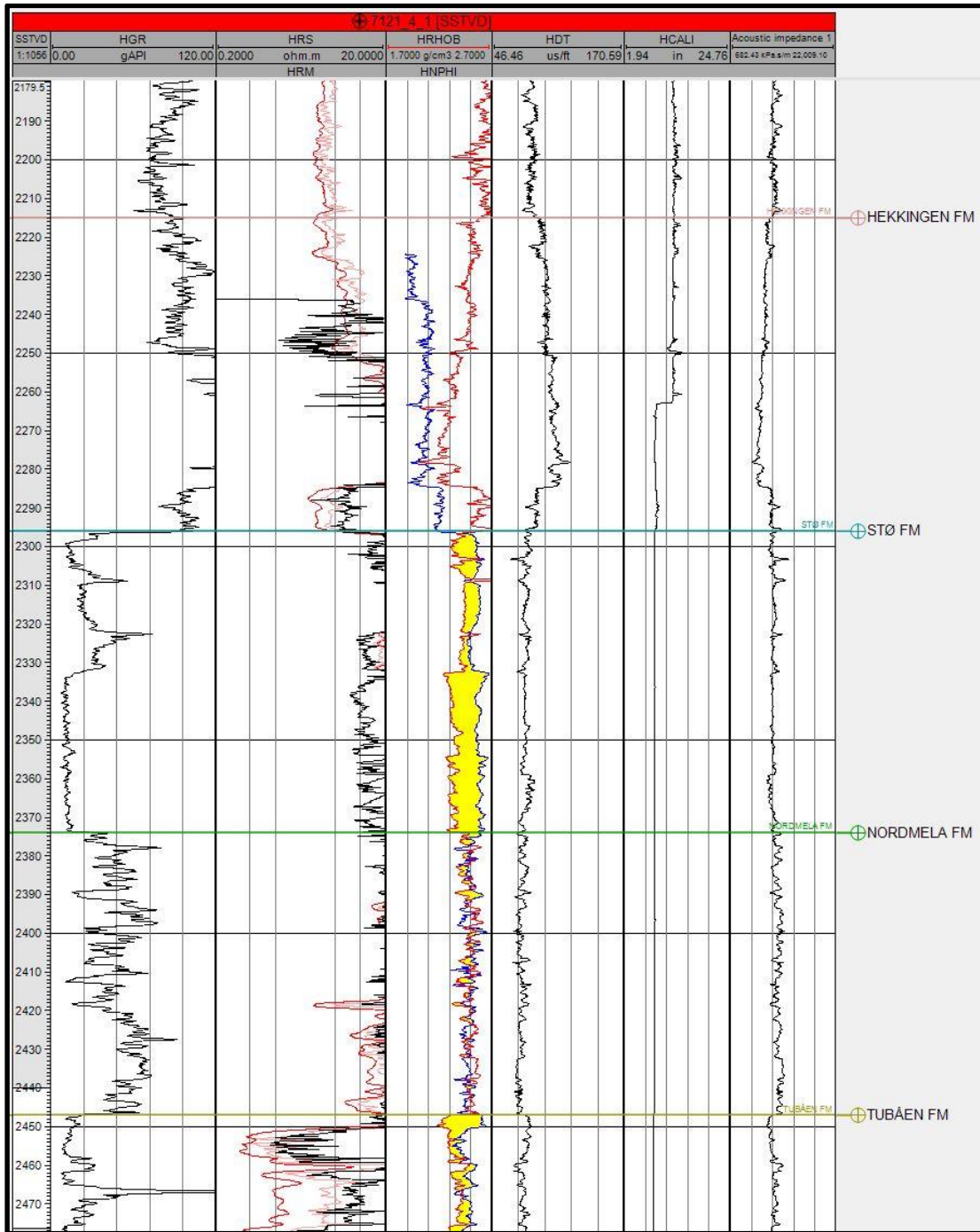


Figure A 7: The composite log in the reservoir interval for the well 7121_4_1.

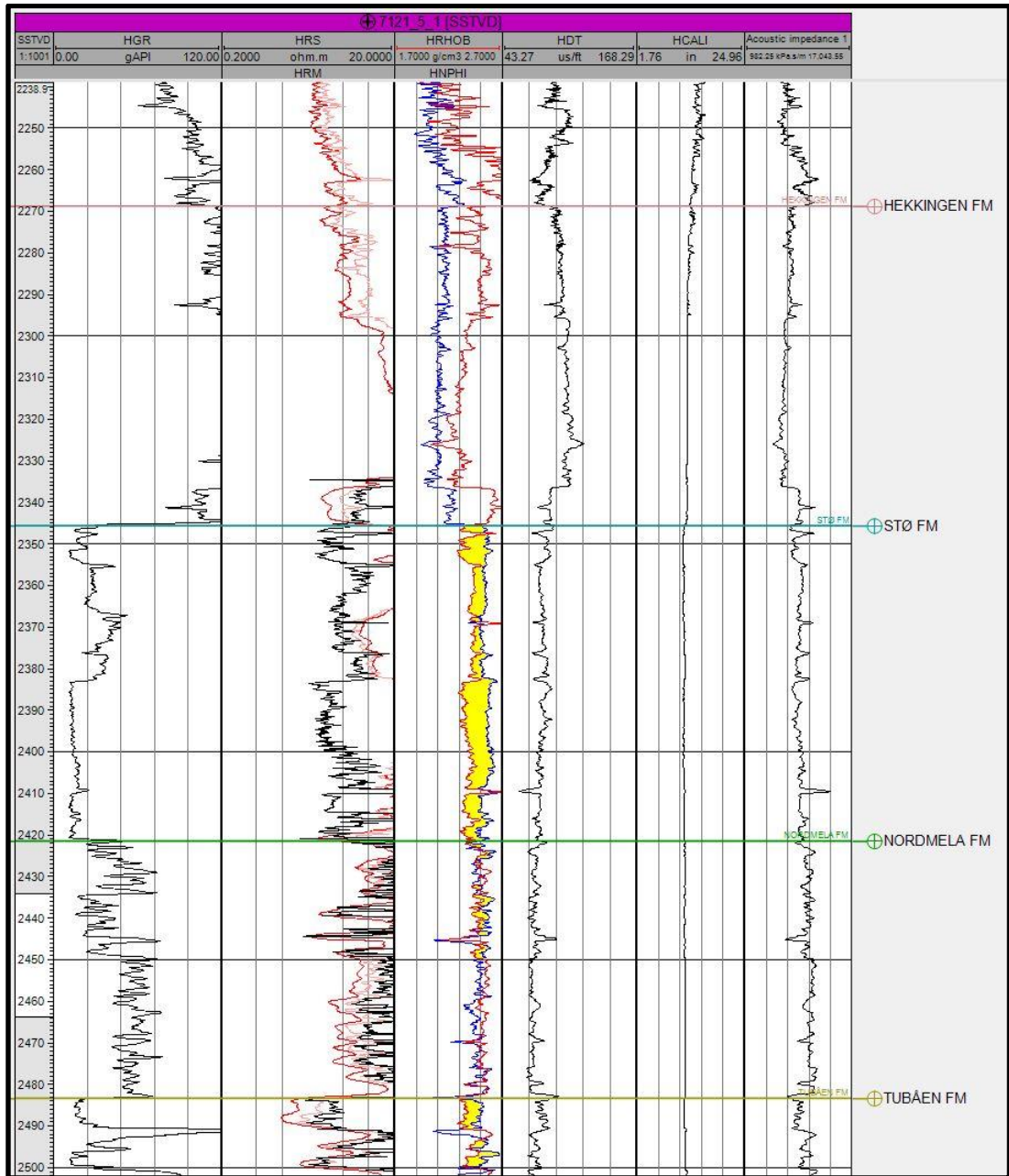


Figure A 8: The composite log in the reservoir interval for the well 7121_5_1.

The Synthetic Seismogram

For all well section window below, in the track 1 is shown the Slowness and Density as input to obtain the reflectivity series (in track 2). The track 3 wavelet has been convolved with the reflectivity series to obtain the synthetic seismogram in track 5. The synthetic seismogram between is compared to the local seismic at the both side of the synthetic seismogram and the result is the correlation in track 6. The interval velocities are displayed in the followed tracks. The amount in time of the interactively shift is displayed as drift in the last track.

Notice the trajectory well, line in red sometimes curved is shown in between the synthetic seimogram.

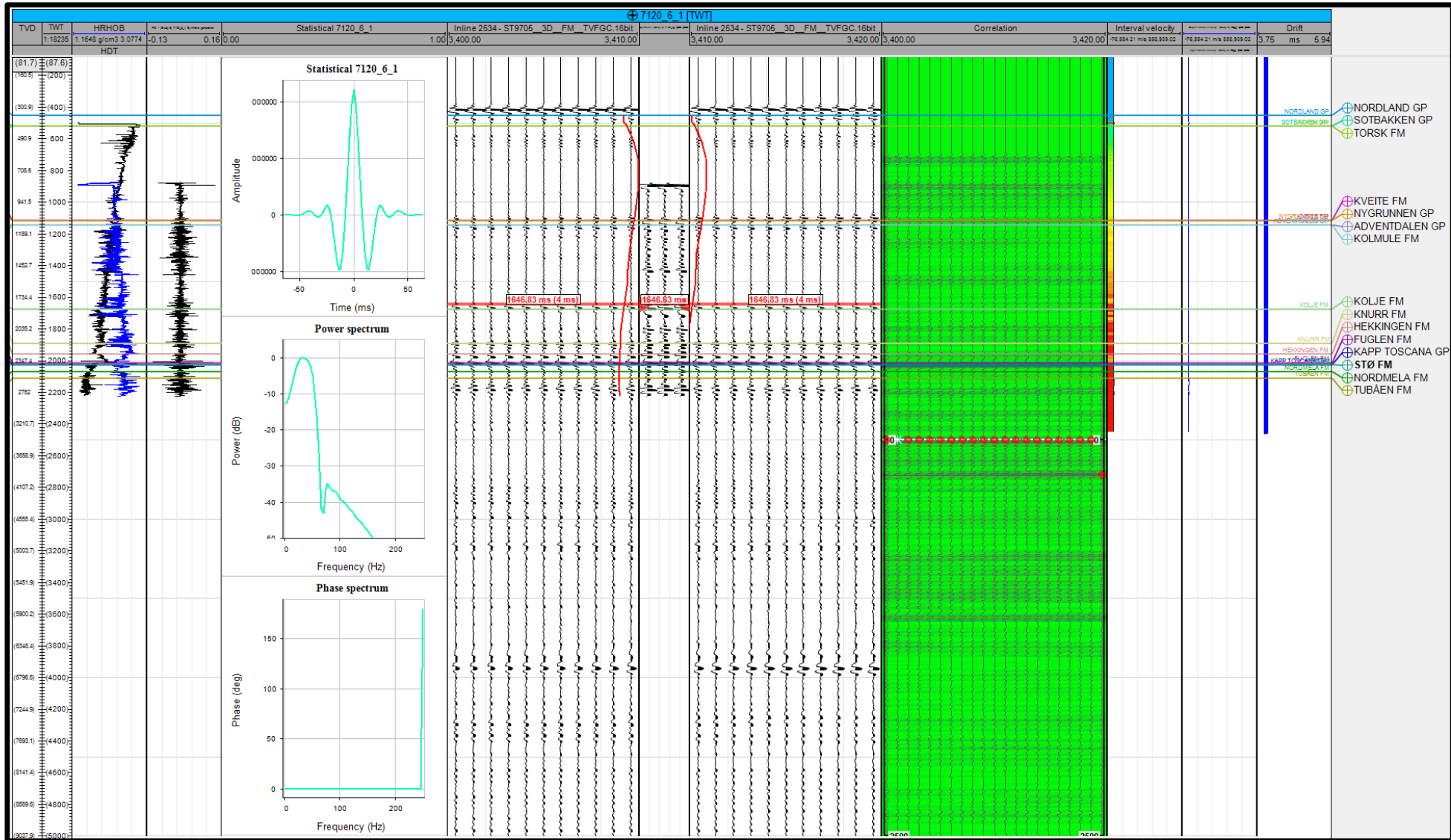


Figure A 10 : Well section window showing synthetic seismogram generated from 7120_6_1 well data and the wavelet obtained from statistical method, the convolution model.

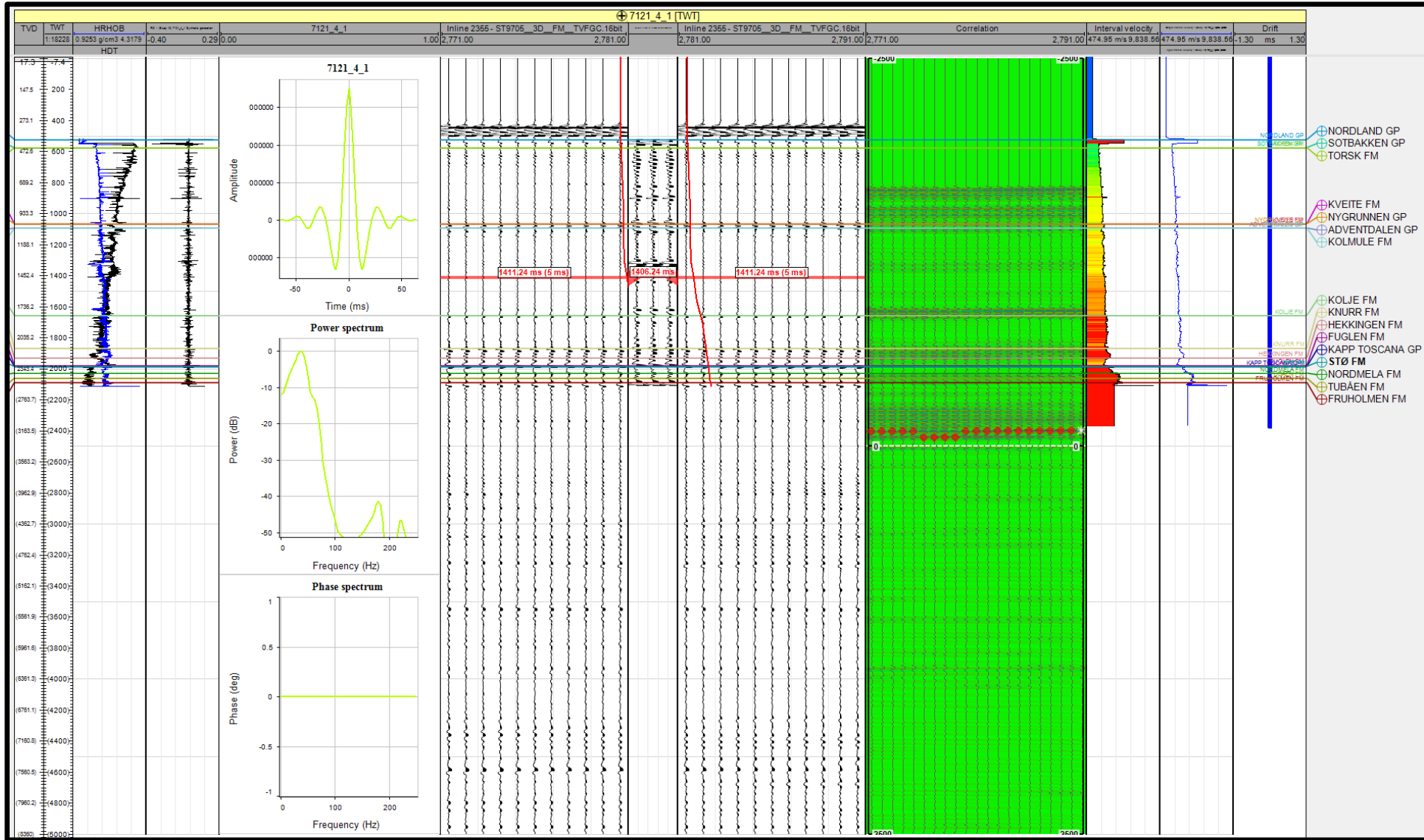


Figure A 11: Well section window showing synthetic seismogram generated from 7121_4_1 well data and the wavelet obtained from statistical method, convolution model

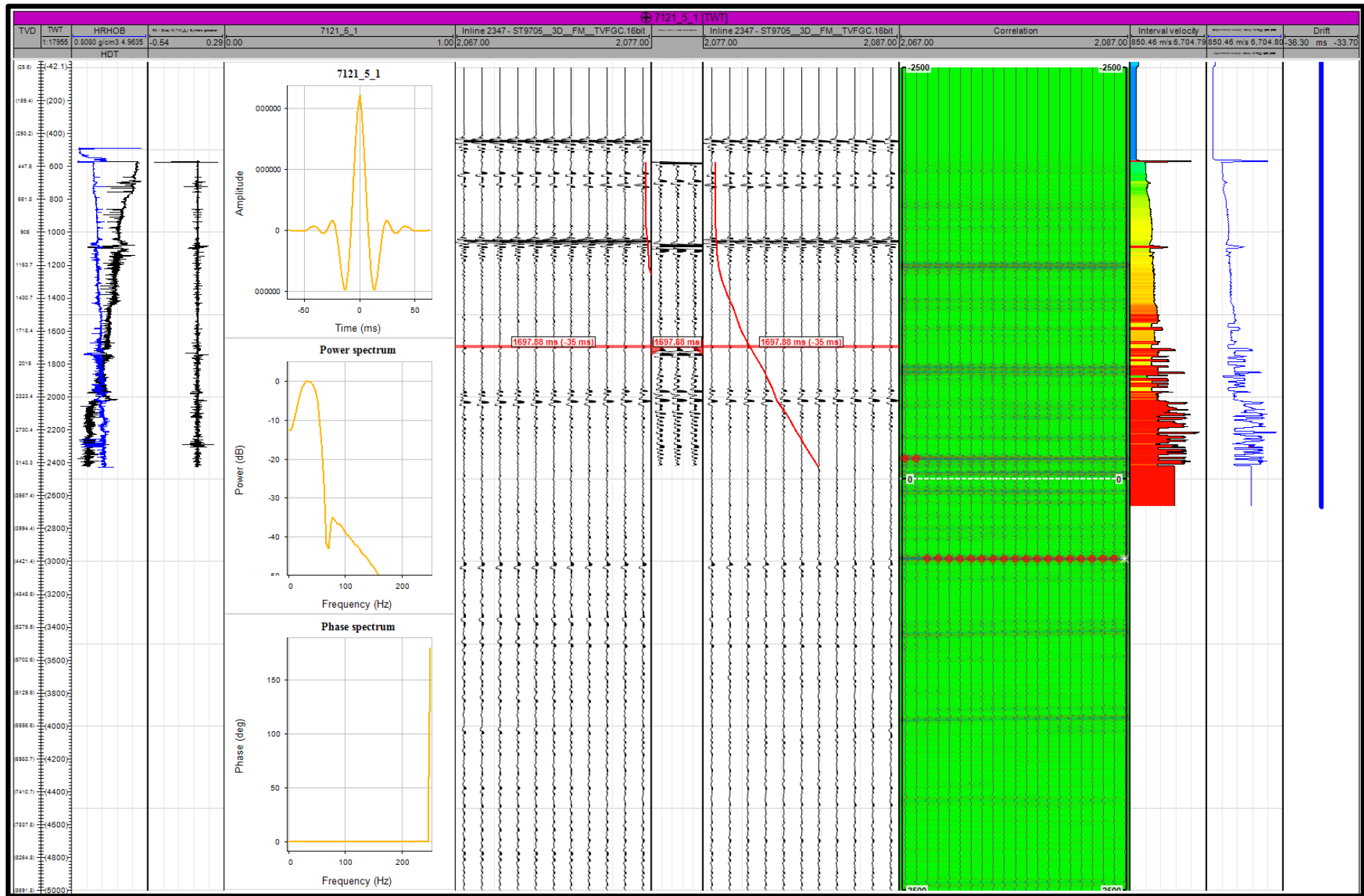


Figure A 12: The well section window showing synthetic seismogram generated from 7121_5_1 well data and the wavelet obtained from statistical method. The red asterisk in the correlation track shows the quality of the correlation within each trace.

The Fluid contacts in the interpreted structures inside the cube

The interpreted fluid level differs from each other in the structures showing that there is no locally contact among them. It reinforces the idea that these structures can be regarded as different.

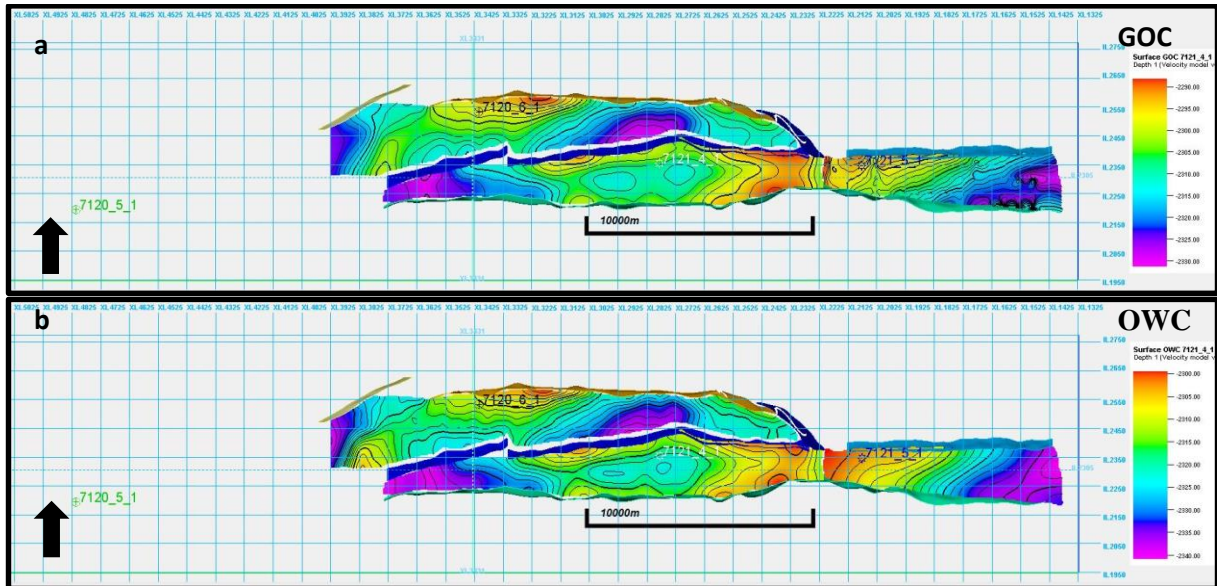


Figure A 13: The fluid contacts for the interpreted e structures containing hydrocarbon